A THESIS

On

EFFECT OF HEAT TREATMENT ON ZnS:Eu NANOPARTICLES: SYNTHESIS AND CHARACTERIZATION

Submitted in the partial fulfillment of requirement for the award of the

Degree of

Master of Science (PHYSICS)

Submitted by: **VAISHALI SINGHI**

Roll No.: 30704020

Under the Guidance of

Dr. N.K.VERMA

Professor and Dean

School of Physics and Materials Science

THAPAR UNIVERSITY

PATIALA (PUNJAB)-147 004

JULY 2009

Dedicated

To

My Parents

CERTIFICATE

This is to certify that the report entitled "**Effect of heat treatment on ZnS:Eu nanoparticles: Synthesis and Characterization**" submitted by **Vaishali Singhi, Roll No. 30704020**, student of M.Sc. (Physics), Thapar University, Patiala, was carried out by her under my supervision. She has not submitted this material for credit towards any other degree at Thapar University, Patiala or at any other University.

(N. K. Verma)

Supervisor

Professor and Dean

School of Physics & Materials Science

Thapar University

Patiala

(O. P. Pandey)

Professor and Head

School of Physics & Materials Science

Thapar University

Patiala

(R. K. Sharma)

Dean of Academic Affairs

Thapar University

Patiala

ACKNOWLEDGEMENT

This piece of work will never be accomplished without our God Almighty with His blessings and His power that work within me and also without the people behind my life for inspiring, guiding and accompanying me through thick and thin.

Foremost, I would like to express my sincere gratitude to my esteemed and worthy supervisor Dr. N. K. Verma, Professor, School of Physics and Materials Science, for the continuous support of my thesis work, for his patience, motivation, enthusiasm, and immense knowledge. His guidance helped me in all the time of research and writing of this thesis. I could not have imagined having a better supervisor and mentor for my thesis.

I shall be failing in my duties if I do not express my deep sense of gratitude towards Dr. O. P. Pandey, Professor and Head, School of Physics and Materials Science, who has been a source of inspiration for me throughout this work.

Besides them, I would like to thank Ms. Zinki Jindal, Mr. Sanjeev Kumar and Mr. Sunil Kumar, Research Scholars, for their encouragement, their timely help, cooperation, useful discussions, hard questions and good wishes. My sincere thanks also goes to all the faculty and staff members of School of Physics and Materials Science for their support and encouragement. I would also, like to thank my friends, who helped me at various stages during the due course of my work.

Last but not the least, I would like to extend my heartfelt gratitude to my parents. My project would not have seen daylight without the immense cooperation and moral support of my parents who kept my spirits up during the endeavor.

Great thanks to all my well wishers.

Vaishali Singhi

(VAISHALI SINGHI)

Abstract

ZnS is an important II-VI, direct band gap semiconductor and is a commercially important having a wide optical band gap, rendering it a very attractive material for optical application especially in nanocrystalline form. ZnS:Eu nanoparticles have been synthesized using chemical precipitation by using water as a solvent. The samples have been heat treated at 200 ^{o}C for 2 hours in nitrogen gas atmosphere and the effect on the structural and optical properties have been studied. The crystal structure and the average crystallite size of the samples have been calculated using X-ray diffraction pattern. The elemental analysis has been carried out by EDX spectroscopy and FTIR spectroscopy. The band gap of ZnS:Eu nanoparticles, with and without heat treatment, has been calculated by UV-Visible absorption spectra. Room temperature PL studies have been carried out to study the emission characteristics of synthesized nanoparticles.

Structural changes have been observed in XRD pattern after heat treatment of the samples. Also the changes have been observed in optical characterization with doping and heat treatment.

Contents

CHAPTER 1

INTRODUCTION

1.1 Nanoscience and Nanotechnology

1.1.1 Introduction

'Nanotechnology' is the relatively new area of science that has generated excitement worldwide. Working at nanoscale, scientists are creating new tools, products and technologies to address some of the world's biggest challenges.

'Nanoscience', is a combination of nano, meaning "dwarf" and the word science. Nanometer refers to 10^{-9} or one billionth of a meter. For comparison, a human hair is 100,000 nm thick. Nanoscience deals with the science of materials and technologies in the scale range of 1-100 nm [1, 2]. This means, the nanoscience deals with a few hundred to a few thousand atoms or atomic clusters, whereas microscopic world is made out of trillions of atoms or molecules. Nanoparticles are larger than individual atom and molecules, but are smaller than bulk solid; hence they obey neither absolute quantum chemistry nor laws of classical physics and have properties that are different from those expected. Physics is different on nanometer scale [3]. Properties not seen on a macroscopic scale are now becoming important on nanoscale such as – quantum mechanics, optics, magnetism, surface reactivity and thermodynamics.

Nanotechnology is the engineering of functional systems at the molecular scale. Nanotechnology is sometimes called as molecular manufacturing and it is the branch of engineering that deals with design and manufacture of extremely small electronic circuits, mechanical devices built at the molecular level of matter. **Nanotechnology is the design characterization, production, and application of structures, devices and systems by controlling shape and size at the nanoscale** [4, 5]**.**

Specialty about the nanoscale is that materials can have different properties at the nanoscale – some are better at conducting electricity or heat, some are stronger, some have different magnetic properties, some reflect light better or change colors as their size is changed [6]. For example, nanomaterials have large surface areas than similar volumes of large scale materials, i.e. large surface is available for interactions with other materials around them.

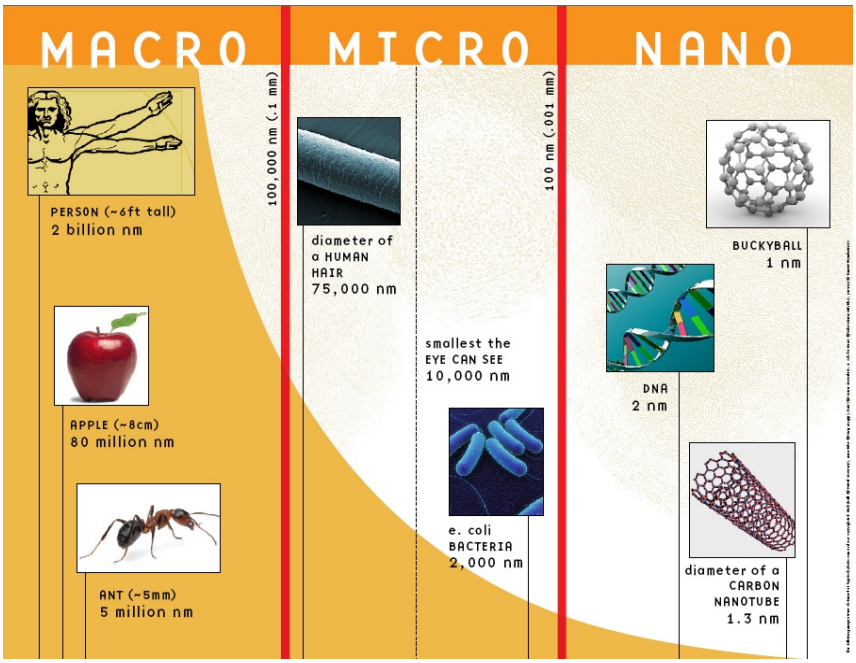

Figure 1.1: Pictorial view of some of the examples of macro, micro and nanoscale objects

1.1.2 The Progression of Nanotechnology

Why now? If it seems that nanotechnology has begun to blossom in the last ten years, this is largely due to the development of new instruments that allow researchers to observe and manipulate matter at the nano-level. Technologies such as scanning tunneling microscopy, magnetic force microscopy, and electron microscopy allow scientists to observe events at the atomic level. At the same time, economic pressures in the electronics industry have forced the development of new lithographic techniques that continue the steady reduction in feature size and cost [5]. As better instrumentation for observing, manipulating and measuring events at this scale are developed, further advances in understanding and ability will occur.

1.1.3 Nanostructures

Nanostructures can be characterized on the basis of the number of dimensions in the nanoscale (1-100 nm) [7] as follows:

2-D nanostructures are confined in one direction e.g., interfaces, membranes, thin films, Multi-layers etc.

1-D nanostructures are confined in two spatial directions e.g., nanowires, nanotubes, DNA etc.

0-D nanostructures are confined in all three spatial directions e.g., nanoparticles, quantum dots etc.

1.1.4 Nanoparticles

Nanoparticles are of great scientific interest as they are effectively a bridge between bulk materials and atomic or molecular structures. A bulk material should have constant physical properties regardless of its size, but at the nano-scale this is often not the case. Size-dependent properties are observed such as quantum confinement in semiconductor particles, surface plasmon resonance in some metal particles [8]. Like a **quantum dot** is a semiconductor whose excitons are confined in all three spatial dimensions. As a result, they have properties that are between those of bulk semiconductors and those of discrete molecules.

The properties of materials change as their size approaches the nanoscale and as the percentage of atoms at the surface of a material becomes significant. For bulk materials larger than one micrometer the percentage of atoms at the surface is minuscule relative to the total number of atoms of the material [9]. The interesting and sometimes unexpected properties of nanoparticles are partly due to the aspects of the surface of the material dominating the properties in comparison to the bulk properties.

Nanoparticles exhibit a number of special properties relative to bulk material. Nanoparticles have a very high surface area to volume ratio. This provides a tremendous driving force for diffusion, especially at elevated temperatures. The large surface area to volume ratio also reduces the incipient melting temperature of nanoparticles [10]. Moreover nanoparticles have been found to impart some extra properties to various day to day products. Like the presence of titanium dioxide nanoparticles impart the self-cleaning effect, and the size being in nanorange, the particles can't be seen. ZnO nanoparticles have been found to have superior UV blocking properties compared to its bulk substitute. That’s why it is often used in the sunscreen lotions.

1.1.5 Quantum Confinement

In any material, substantial variation of fundamental electrical and optical properties with reduced size will be observed when the energy spacing between the electronic levels exceeds the thermal energy (kT).

In small nanocrystals, the electronic energy levels are not continuous as in the bulk but are discrete (finite density of states), because of the confinement of the electronic wave function to the physical dimensions of the particles. This phenomenon is called quantum confinement and therefore nanocrystals are also referred to as **quantum dots (QDs)**. The **quantum confinement** effect can be observed once the diameter of the particle is of the magnitude as the wavelength of electron wave function. When the materials are so small, their electronic and optical properties deviate substantially from those of bulk materials.

A particle behaves as if it were free when the confining dimension is large compared to the wavelength of the particle [11]. During this state, band gap remains at its original energy due to continuous energy state. However, as the confining dimension decreases and reaches a certain limit, typically in nanoscale, the energy spectrum turns to discrete. As a result, band gap becomes size dependent. This ultimately results to a blue shift in optical illumination as the size of the particles decreases.

Specifically, the effect describes the phenomenon results from electrons and electron holes being squeezed into a dimension that approaches a critical quantum measurement, called the exciton Bohr radius.

Quantum confinement describes the increase in energy which occurs when the motion of a particle is restricted in one or more dimensions by a potential well. When the confining dimension is large as compared to the wavelength of the particle, the particle behaves as if it were free. As the confining dimension decreases, the particle's energy increases. A quantum dot [12] is a well that confines in all three dimensions such as a small sphere, a quantum wire confines in two dimensions, and quantum well confines in one dimension.

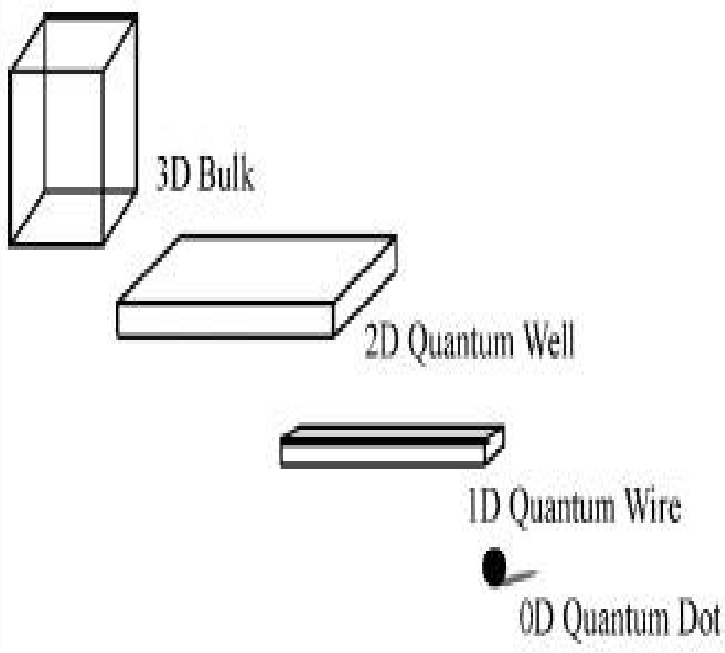

Figure 1.2: Picture of different dimensional structures

1.1.6 Surface Area to Volume Ratio

Surface area to volume ratio (SA/V) is one of the key concepts for the understanding of nanoscale science and technology. SA/V is a prerequisite to understanding size-dependent properties and behaviors and changes that are at the core of nanoscience. Not only the size of objects or systems changes with scale, but also the way in which they function or behave also reflects the changes. For example, even small changes in linear size yield larger relative changes in area, and even larger changes in volume. Thus, if a property is dependent on volume (e.g., heat capacity, mass), then it will change much faster than properties dependent on area (e.g., cooling surface, absorptivity) for a given change in size [13]. Many of the special properties that matter exhibits on the nanoscale result from the effect of size on the surface area to volume ratio (SA/V). When the reactions takes place at the surface of a chemical or material, the greater the surface area to volume ratio the greater the reactivity.

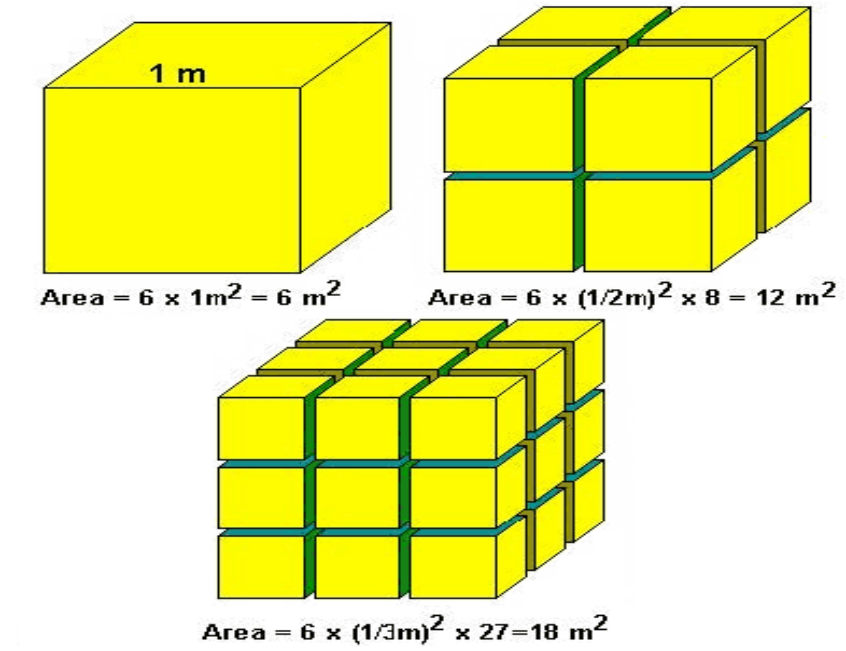

Figure 1.3: Example to illustrate increase in Surface to volume ratio

Nanoparticles are special and interesting because their chemical and physical properties are different from their macro particles. One example of surface area to volume ratio at nanoscale is gold as a nanoparticle. At the macro scale, gold is an inert element i.e. it does not react with many chemicals, whereas at the nanoscale, gold nanoparticles become extremely reactive and can be used as catalysts to speed up reactions.

1.2 Semiconductor Nanoparticles

Almost all materials system including metal, insulators and semiconductors show size dependent electronic or optical properties in the quantum size regime. Among these, the modification in the energy band gap of semiconductors is the most attractive one because of the fundamental as well as technological importance [14]. Semiconductors with widely tunable energy band gap are considered to be the materials for next generation flat panel displays, photovoltaic, optoelectronic devices, laser, sensors, photonic band gap devices, etc. When dimension of a

material is continuously reduced from macroscopic size to nanometers, the physical and chemical properties drastically change.

Semiconductors derive their great importance from the fact that their electrical conductivity can be greatly altered via an external stimulus (voltage, photon flux, etc), making semiconductors critical parts of many different kinds of electrical circuits and optical applications [15]. Optical properties of the quantum dots can be easily tuned with the particle size [16]. The band gap can be controlled with the change in size of the nanomaterial, so the different colored emission can be observed from the same material. These quantum dots of same material can be used for fabrication of LEDs having emission over the whole visible spectrum.

1.3 Properties of Nanomaterials

In nanoparticles, the properties (physical, chemical, biological etc.) can be selectively controlled by engineering the size, morphology, and composition of the particles. Nanomaterials are known to exhibit markedly different properties compared to micron sized ones. These new substances will have enhanced or entirely different properties from their bulk counterparts [17].

Two principal factors cause the properties of nanomaterials to differ significantly from other materials: increased relative surface area, and quantum effects. These factors can change or enhance properties such as reactivity, strength and electrical characteristics. As growth and catalytic chemical reactions occur at surfaces, this means that a given mass of material in nanoparticulate form will be much more reactive than the same mass of material made up of larger particles [18].

It has been shown that the various material properties such as electrical, mechanical, optical, magnetic etc are highly influenced by the fine-grained structure and there is generally improvement in the concerned properties. Using a variety of synthesis methods, it is possible to produce nanostructured materials in the various forms like: thin films, powder, quantum wires, quantum wells, quantum dots, etc.

Nanocrystalline systems have attracted much interest for their novel optical properties, which differ remarkably from bulk crystals. Because of quantum confinement of electrical carriers within nanoparticles, efficient energy and charge transfer over nanoscale distances and in many

systems a highly enhanced role of interfaces [19]. Nanocrystalline materials are exceptionally strong, hard, and, ductile at high temperature, wear-resistance and chemically very active. Nanocrystalline materials are also much more formable than their conventional, commercially available micron counterparts.

1.4 Techniques for Synthesis of Nanoparticles

Nanomaterials are not simply another step in the miniaturization of materials. They often require very different production approaches. There are several processes to create nanomaterials. Two main approaches are used in nanotechnology. In the "top-down" approach, nano-objects are constructed from larger entities without atomic-level control. In the "bottom-up" approach, materials and devices are built from molecular components which assemble themselves chemically by principles of molecular recognition.

The **top-down** approach often uses the traditional workshop or micro fabrication methods where externally-controlled tools are used to cut, mill and shape materials into the desired shape and order. Micro patterning techniques, such as photolithography and inkjet printing belong to this category.

Figure 1.4: Top down Approach

The biggest problem with top-down approach is the imperfection of the surface structure. The conventional top-down techniques such as lithography can cause significant crystallographic damage to the processed patterns, and additional defects may be introduced even during the etching steps [20]. For example, nanowires made by lithography are not smooth and may contain

a lot of impurities and structural defects on the surface. Such imperfections would have a significant impact on physical properties and surface chemistry of nanostructures and nanomaterials, since the surface over volume ratio in nanostructures and nanomaterials is very large. The surface imperfection would result in a reduced conductivity due to inelastic surface scattering, which in turn would lead to the generation of excessive heat and thus impose extra challenges to device design and fabrication.

Bottom-up approaches use the chemical properties of single molecules to cause single-molecule components to (a) self-organize or self-assemble into some useful conformation, or (b) rely on positional assembly. These approaches utilize the concepts of molecular self-assembly and/or molecular recognition. Such bottom-up approaches should be able to produce devices in parallel and much cheaper than top-down methods, but could potentially be overwhelmed as the size and complexity of the desired assembly increases.

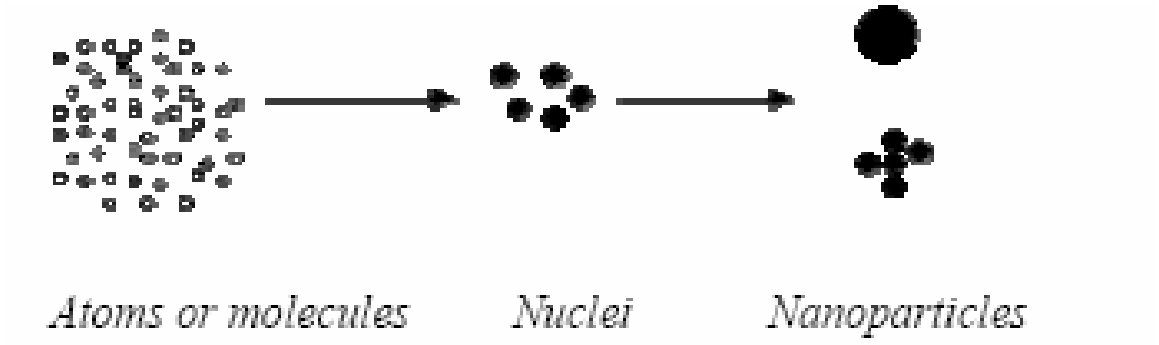

Figure 1.5: Bottom-up Approach

Bottom-up approach refers to the build-up of a material from bottom: atom-by-atom, molecule-by-molecule, or cluster-by-cluster. In crystal growth, growth species, such as atoms, ions and molecules, after impinging onto the growth surface, assemble into crystal structure one after another. For most materials, there is no difference in physical properties of materials regardless of the synthesis routes, provided that chemical composition, crystallinity, and microstructure of the material are identical [21]. Of course, different synthesis and processing approaches often result in appreciable differences in chemical composition, crystallinity, and microstructure of the

material due to kinetic reasons. Consequently, the material exhibits different physical properties. Although the bottom-up approach is not new, it plays an important role in the fabrication and processing of nanostructures and nanomaterials. There are several reasons for this. When structures fall into a nanometer scale, there is little choice for top-down approach.

Bottom-up approach also promises a better chance to obtain nanostructures with less defects, more homogeneous chemical composition, and better short and long range ordering. This is because the bottom-up approach is driven mainly by reduction of Gibbs free energy, so that nanostructures and nanomaterials such produced are in a state closer to a thermodynamic equilibrium state. On the contrary, top-down approach most likely introduces internal stress, in addition to surface defects and contaminations.

1.5 Applications of Semiconducting Nanoparticles

Nanocrystalline semiconductors have been the subject of numerous investigations in the past two decades. If the semiconductor particles become smaller than the Bohr radius of the exciton, quantum size effects occur. As a result of these quantum size effects, the band gap of the semiconductor increases and at the edges of the valence and conduction band discrete energy levels occur [22]. On the other hand, the surface states will play a more important role in the nanoparticles, due to their large surface-to-volume ratio with a decrease in particle size. In the case of semiconductor nanoparticles, radiative or non-radiative recombination of an exciton at the surface states becomes dominant in its optical properties with a decrease of particle size. Therefore, the decay of an exciton at the surface states will influence the qualities of the material for an optoelectronic device. These size dependent optical properties have many potential applications in the areas of solar energy conversion, light emitting devices, chemical/biological sensors and photocatalysis [23]. Wide band gap II–VI semiconductors are expected to be the novel materials for the optoelectronic devices. ZnS, which is an important member of this family, has been extensively investigated as it has numerous applications. ZnS has been used widely as an important phosphor for photoluminescence (PL), electroluminescence (EL) and cathodoluminescence (CL) devices due to its better chemical stability compared to other chalcogenides. In optoelectronics, it finds use as light emitting diode, reflector, dielectric filter and window material. Among the family of II–VI semiconductors, ZnS, CdS, ZnO, CdTe, etc. are the foremost candidates because of their favorable electronic and optical properties for

optoelectronic applications. ZnS has been used for the cathode ray tube, the field emission display, and the scintillator, as one of the most frequently used phosphors. In addition, a ZnS crystal laser has been produced using streamer excitation, and thin films of ZnS can be used as an active emitting material in such a device, termed the hot electron cold cathode.

1.6 Literature Review

During the past decade, the preparation and characterization of materials on the nanometer scale has provided not only new physics in reduced dimensions, but also the possibility of fabricating novel materials. ZnS and CdS are omnipresent scale semiconductor materials and are commercially used in photoluminescence (PL) and electroluminescence applications. Doped nanocrystals (DNC) of semiconductors are a new class of luminescent materials. Nanocrystals doped with optically active luminescence centers create new opportunities for luminescence research and also for the application of nanometer-scale structured material [24]. Bhargava reported manganese doped ZnS nanocryatals in 1994 [25]. They pointed out that carriers can recombine via luminescence centers and exhibit very short lifetime in DNC compared to the analogous bulk materials. However, other researchers found that the lifetimes of luminescence centers both in bulk and in nanocrystalline materials are almost at the same order. Thus DNC's are worth investigating in more details because band gap of nanocrystalline hosts can be adjusted by sizes to match the energy levels of luminescent centers and thus new luminescence is expected. Moreover, nanocrystalline materials can be prepared at rather low temperature (for example 100 ^{o}C) with respect to conventional phosphor materials synthesized at high temperature over 1000 °C. Recent studies [26] have revealed that rare-earth-doped luminescent II-VI materials are promising candidates for applications in color thin-film EL devices. In general, the luminescence of rare-earth-doped systems mainly reflects the properties of the dopant. However, in this system, the luminescence of ZnS nanoparticles was preserved and, even more, its intensity was greatly enhanced when Eu^{3+} was introduced in the ZnS polymer matrix. The exciton Bohr radius of II-VI semiconductors is larger (e.g., 2.5 nm for CdS) resulting in pronounced quantum confinement effects for nanoparticles of about 2.5 nm and smaller. Therefore, a possible influence of quantum size effects on the luminescence properties of RE ions is only expected in II-VI semiconductor nanocrystals. A number of papers reported on the luminescence of nanocrystalline II-VI semiconductors doped with Tb^{3+}, Sm^{2+}, Eu^{3+}/Eu^{2+}, or Er.

In this report, the incorporation of RE ions in nanocrystalline ZnS and CdS is investigated in a systematic way [27, 28]. Old and new synthesis methods are used and compared. Besides room-temperature preparation methods, post synthesis heat treatment (up to 800 °C) was done to promote incorporation of RE ions in ZnS or CdS nanoparticles. Even ion implantation was attempted as a method to incorporate RE ions in semiconductor nanoparticles. From careful luminescence studies, it is concluded that with the preparation techniques applied, it is not possible to incorporate RE ions in nanocrystalline semiconductors. ZnS has been used widely as an important phosphor for photoluminescence (PL), electroluminescence (EL) and cathodoluminescence (CL) devices due to its better chemical stability compared to other chalcogenides such as ZnSe. Doping of ZnS nanoparticles by transition metal ions e.g. Mn^{2+}, Cu^{2+} and rare earth ions e.g. Eu^{2+} have been successfully done by techniques such as thermal evaporation, sol-gel processing, co-precipitation, micro emulsions, etc [29]. These doped ZnS semiconductor materials have a wide range of applications in electroluminescence devices, phosphors, light emitting displays, and optical sensors. Accordingly, study of luminescence properties of ZnS has received special attention. In addition to the blue luminescence of ZnS host, emission in different visible bands related to various dopants has been reported by Jayanthi et. al. [30]. This includes orange luminescence in ZnS:Mn nanoparticles, attributed to the $4T^1$-$6A^1$ transition of Mn^{2+} ions excited via energy transfer from the host ZnS, red emission from the characteristic $4f^7$-$4f^6 5d^1$ transition of Eu^{2+} in ZnS:Eu nanoparticles and green luminescence in ZnS:Cu. Rare-earth (RE) ions as dopants should be more interesting in modifying its photoluminescence (PL) properties considering the special $4f$ –$4f$ intra-shell transitions in RE ions [31,32]. Until now, there have been rare reports on the preparation of stable RE ion-doped II–VI compound semiconductor nanocrystals because they are trivalent charged with larger radii. Although Eu^{3+}-doped ZnS nanoparticles embedded in polymer matrix have been reported to be available in which Eu^{3+} ions were found both in the polymer matrix and on the surface of ZnS nanocrystal, the preparation of free-standing Eu^{3+}-ZnS nanocrystals that exhibit high quality luminescence properties is still a problem, because doping will bring out surpass charges as well as lattice distortion when trivalent RE ions enter in the ZnS crystal lattice. In this letter, we report the synthesis, characterization, and photoluminescence properties of stable free-standing ZnS:Eu^{3+} nanocrystals prepared in a water/methanol solution [33]. Recently, it was suggested that quantum confinement can modify the energy structure of doped nanoparticles and change

the relative energy positions of the dopants. We also demonstrated that quantum confinement can move the excited states of Eu^{2+} into the energy gap of ZnS in nanoparticles, and thus enables the intra-ion transition of Eu^{2+} in ZnS nanoparticles. Chen et. al. mainly discussed the size dependence of Eu^{2+} fluorescence in ZnS:Eu^{2+} nanoparticles [34]. Here the fluorescence size dependence of ZnS:Eu^{2+} nanoparticles was observed, and possible mechanisms for the shift of the Eu^{2+} intra-ion $4f^{6}5d^{1}(t_{2g})$–$4f^{7}$ emission were discussed. It was concluded that the decrease in the electron phonon coupling and the crystal field strength is the major factor responsible for the shift of Eu^{2+} intra-ion emission to higher energies for smaller nanoparticles.

In our present study, we have synthesized and studied various properties of ZnS nanoparticles, doped with Europium, by varying the concentration of Europium, which has been discussed in chapter 3, and then by providing heat treatment to the samples at 200 ^{o}C for 2 hours in nitrogen gas atmosphere.

CHAPTER 2

MATERIALS AND CHARACTERIZATION

2.1 Materials

2.1.1 Introduction

Wide band gap II–VI semiconductors are expected to be the novel materials for the optoelectronic devices. ZnS is an important member of this family and it has been extensively investigated [35] as it has numerous applications to its credit. ZnS has been used widely as an important phosphor for photoluminescence (PL), electroluminescence (EL) and cathodoluminescence (CL) devices due to its better chemical stability compared to other chalcogenides such as ZnSe. ZnS is a commercially important II–VI semiconductor having a wide optical band gap, rendering it a very attractive material for optical application especially in nanocrystalline form. ZnS can have two different crystal structures (zinc blende and wurtzite), both of which are direct band structure [36, 37]. ZnS has been used for the cathode ray tube, the field emission display, and the scintillator as one of the most frequently used phosphors. In addition, a ZnS crystal laser has been produced using streamer excitation, and thin films of ZnS can be used as an active emitting material in such a device, termed the hot electron cold cathode. In optoelectronics, it finds use as light emitting diode, reflector, dielectric filter and window material. Keeping in view the above discussion, an effort has been made to study the optical properties of ZnS nanoparticles of different sizes.

2.1.2 Properties of ZnS

ZnS occurs in two common polytypes, zincblende (also called sphalerite) and wurtzite. The two types have these features in common:

- 1:1 stoichiometry of Zn:S
- a coordination of 4 for each ion (4:4 coordination)
- tetrahedral coordination

Zinc blende/ sphalerite is based on a fcc lattice of anions whereas wurtzite is derived from an hcp array of anions [38]. In both structures, the cations occupy one of the two types of tetrahedral holes present. In either structure, the nearest neighbor connections are similar, but the distances

and angles to further neighbors differ. Zinc blende has 4 asymmetric units in its unit cell whereas wurtzite has 2.

Zinc blende is best thought of as a face-centered cubic array of anions and cations occupying one half of the tetrahedral holes. Each ion is 4-coordinate and has local tetrahedral geometry [39]. Unlike wurtzite, zincblende is its own antitype -- we can switch the anion and cation positions in the cell (as in NaCl). In fact, replacement of both the Zn and S with C gives the diamond structure.

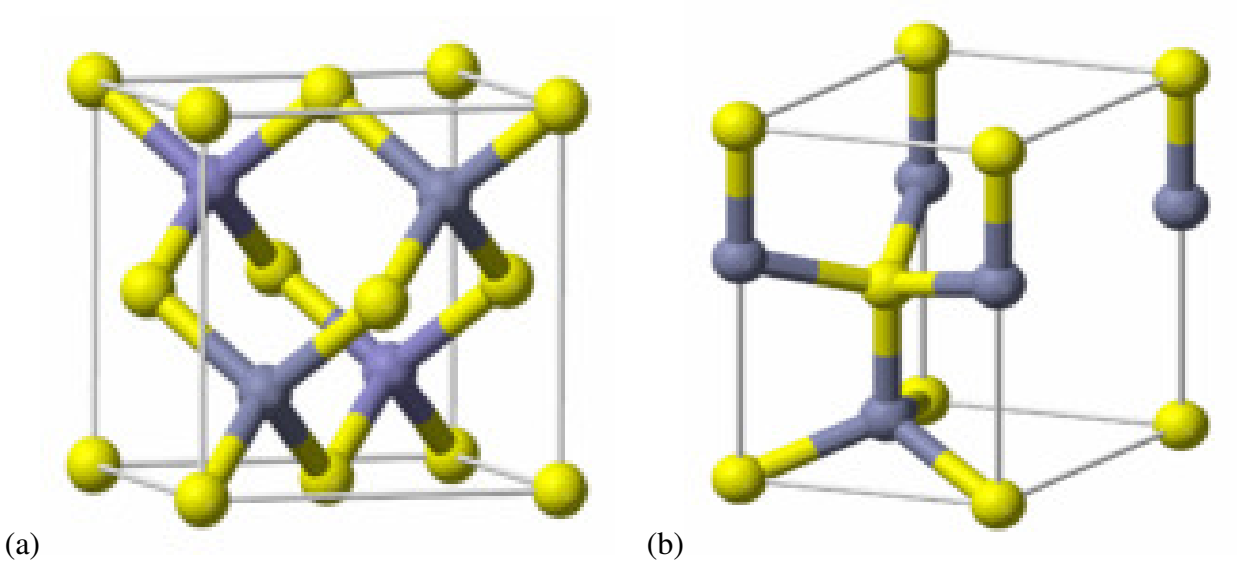

(a) (b)

Figure 2.1: (a) Sphalerite (Cubic with band gap 3.54 eV) **(b)** Wurtzite (Hexagonal with band gap 3.67 eV)

Table 2.1: Zinc blende Vital Statistics

Formula	ZnS
Crystal System	Cubic
Lattice-Type	Face-centred

Cell Parameters	a = 5.41 Å, Z=4
Atomic Positions	S: 0, 0, 0 Zn: 0.25, 0.25, 0.25
Density	4.102 $g.cm^{-3}$
Melting Point	phase transition at 1020 degrees C
Alternate Names	Zinc blende, Sphalerite

2.1.3 Doping

2.1.3.1 Doping in nanoparticles

Intrinsic semiconductors need to be doped to modify their properties. The maximum doping normally used in bulk is of the order of one dopant atom per 10^5 atoms. Doping nanocrystals at such levels is unrealistic as their nuclearity is often below 10^5 atoms. Furthermore, nanocrystals possess a different band structure as well as excitonic character due to quantum confinement. Semiconductor nanocrystals are doped with few percent of impurities to create impurity centers that interact with electrons and holes. A useful effect of this interaction is that the mid gap states arising from surface species can be shifted outside the gap region. Dopants do not affect the absorption spectra however, emission intensity is greatly increased. Doping is achieved by simply introducing the dopant in the reacting mixture. It was suggested that success of doping is related to the binding energy of the dopant ions to the exposed surface of the growing nanocrystal. High binding energies lead to successful adsorption and doping, while low binding energies means that doping is unfavoured.

Semiconductors, in nanocrystallized form, exhibit markedly different electrical, optical and structural properties as compared to those in the bulk form [40]. Out of these, the ones suited as phosphor host material show considerable size dependent luminescence properties when an impurity is doped in a quantum-confined structure. The impurity incorporation transfers the dominant recombination route from the surface states to impurity states. If the impurity-induced transition can be localized as in the case of the transition metals or the rare earth elements, the radiative efficiency of the impurity-induced emission increases significantly. The emission and

decay characteristics of the phosphors are, therefore, modified in nanocrystallized form. Also, the continuous shift of the absorption edge to higher energy due to quantum confinement effect, imparts these materials a degree of tailorability. Obviously, all these attributes of a doped nanocrystalline phosphor material are very attractive for optoelectronic device.

2.1.3.2 Doping of Rare-earth ions

It is known that rare earth (RE) elements are effective luminescent centers. RE-doped luminescent II-VI materials, for example, Eu, Ce and Sm doped CaS and SrS, are promising candidates for application in color thin-film electroluminescence devices. But the instability and hygroscopic nature of CaS and SrS are problems in their application. Whereas, ZnS is more stable than CaS or SrS as host of luminescent materials.

The exciton Bohr radius of II-VI semiconductors is larger resulting in pronounced quantum confinement effects for nanoparticles of about 2.5 nm and smaller. Therefore, a possible influence of quantum size effects on the luminescence properties of RE ions is only expected in II-VI semiconductor nanocrystals [41]. A number of papers reported on the luminescence of nanocrystalline II-VI semiconductors doped with Tb^{3+}, Sm^{2+}, Eu^{3+}/Eu^{2+}, or Er.

The ionic radii of RE ions are much larger than that for Zn^{2+} (viz., Eu^{3+} = 0.95 and Zn^{2+} = 0.75 Å). If one assumes that the RE ion is incorporated on a Zn^{2+} lattice site, like Mn^{2+} ions in nanocrystalline ZnS:Mn, the ZnS host lattice has to deform locally. In addition, the 3+ charge of a RE ion on a 2+ site has to be compensated for somewhere in the host lattice. Finally, the differences in chemical properties between Zn^{2+} and RE^{3+} will not favor substitution of Zn^{2+} by RE^{3+}. Still, it is known that RE ions can be incorporated in bulk II-VI semiconductors. Efficient luminescence from intraconfigurational $4f^n$-$4f^n$ transitions has been observed for RE ions in bulk ZnS upon excitation over the band gap. However, high temperatures (900- 1200 °C) are needed to accomplish this.

2.1.4 Properties of Europium

Europium is the most reactive of the rare earth elements; it rapidly oxidizes in air, and resembles calcium in its reaction with water; samples of the metal element in solid form, even when coated with a protective layer of mineral oil, are rarely shiny. Europium ignites in air at about 150 °C to 180 °C. It is as hard as lead and quite ductile. Europium is a metal and becomes a superconductor under pressure 80 GPa at temperature 1.8 K.

Europium is one of the less abundant rare-earth elements. It is never found in nature as the free element, but there are many elements containing europium [42, 43]. Europium is a neutron adsorber, so it is used in nuclear reactors control rods. Europium phosphors are used in television tubes to give a bright red color and as an activator for yttrium-based phosphors. For powerful street lighting a little europium is added to mercury vapour lamps to give a more natural light. A salt of europium is used for newer phosphorescent powder and paints.

Figure 2.2: Europium

Europium (II) compounds tend to predominate, in contrast to most lanthanides: (which generally form compounds with an oxidation state of +3). Europium (II) chemistry is very similar to barium (II) chemistry, as they have similar ionic radii. Divalent europium is a mild reducing agent, such that under atmospheric conditions, it is the trivalent form that predominates

Table 2.2: General properties of Europium

Name, Symbol, Number	europium, Eu, 63
Element category	Lanthanides
Appearance	Silvery White
Standard atomic weight	151.964 $g \cdot mol^{-1}$
Electronic configuration	[Xe] $4f^7$ $6s^2$
Phase	Solid
Density	5.264 $g \cdot cm^{-3}$
Melting point	1099ºK
Boling point	1802ºK

2.2 Characterization Techniques

2.2.1 X-Ray Diffraction

X-ray diffraction (XRD) is a versatile, non-destructive technique that reveals detailed information about the chemical composition and crystallographic structure of natural and manufactured materials.

Bragg's law:

When a crystal is bombarded with X-rays of a fixed wavelength and at certain incident angles, intense reflected X-rays are produced when the wavelengths of the scattered X-rays interfere

constructively. In order for the waves to interfere constructively, the differences in the travel path must be equal to integeral multiples of the wavelength [44]. When this constructive interference occurs, a diffracted beam of X-rays will leave the crystal at an angle equal to that of the incident beam.

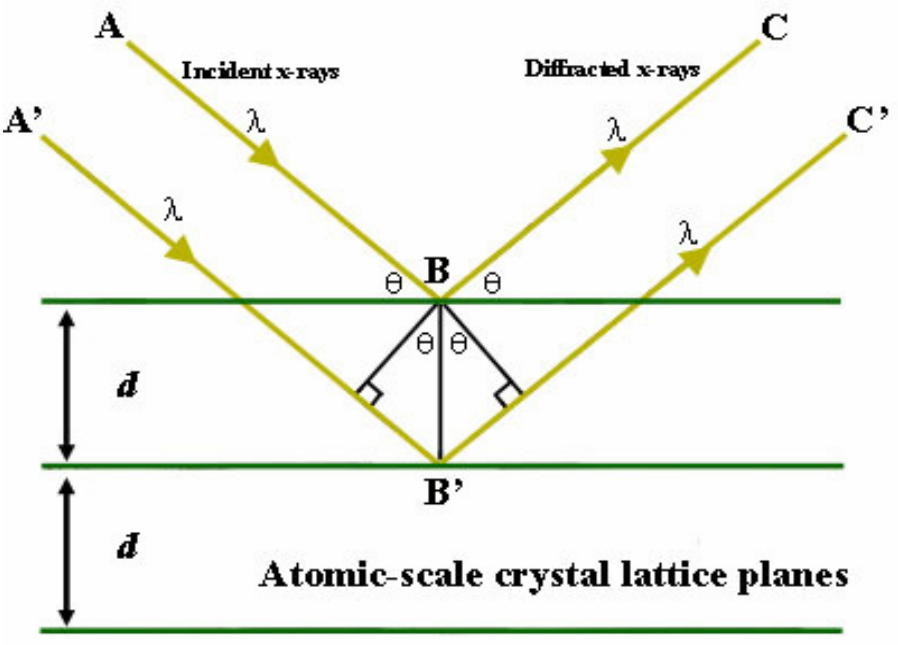

Figure 2.3: Bragg's Law reflection. The diffracted x-rays exhibit constructive interference when the distance between paths ABC and A'B'C' differs by an integer number of wavelengths (λ).

To illustrate this feature, consider a crystal with crystal lattice planar distances d. Where the travel path length difference between the ray paths ABC and A'B'C' is an integer multiple of the wavelength, constructive interference will occur for a combination of that specific wavelength, crystal lattice planar spacing and angle of incidence (θ). Each rational plane of atoms in a crystal will undergo refraction at a single, unique angle (for X-rays of a fixed wavelength).

The general relationship between the wavelengths of the incident X-rays, angle of incidence and spacing between the crystal lattice planes of atoms is known as Bragg's Law. i.e.,

$$n\lambda = 2dSin\theta \qquad \text{--- (2.1)}$$

Where n (an integer) is the "order" of reflection, λ is the wavelength of the incident X- rays, d is the interplanar spacing of the crystal and θ is the angle of incidence.

X-Ray Powder Diffraction (XRD) is an efficient analytical technique used to identify and characterize unknown crystalline materials [45]. Monochromatic X-rays are used to determine the interplanar spacing of the unknown materials. Samples are analyzed as powders with grains in random orientations to insure that all crystallographic directions are "sampled" by the beam. When the Bragg conditions for constructive interference are obtained, a "reflection" is produced, and the relative peak height is generally proportional to the number of grains in a preferred orientation.

Figure 2.4.Bruker's X-ray Diffraction D8-Discover instrument.

The X-ray spectra generated by this technique, thus, provide a structural fingerprint of the unknown. Mixtures of crystalline materials can also be analyzed and relative peak heights of multiple materials may be used to obtain semi-quantitative estimates of abundances. A glancing X-ray beam may also be used to obtain structural information of thin films on surfaces. In

addition, changes in peak position that represent either compositional variation (solid solution) or structure-state information (e.g. order-disorder transitions, resolution, etc.) are readily detectable.

Peak positions are reproducible to 0.02 degree. Peak positions occur where the X-ray beam has been diffracted by the crystal lattice. The unique set of d-spacing derived from this pattern can be used to 'fingerprint' the mineral.

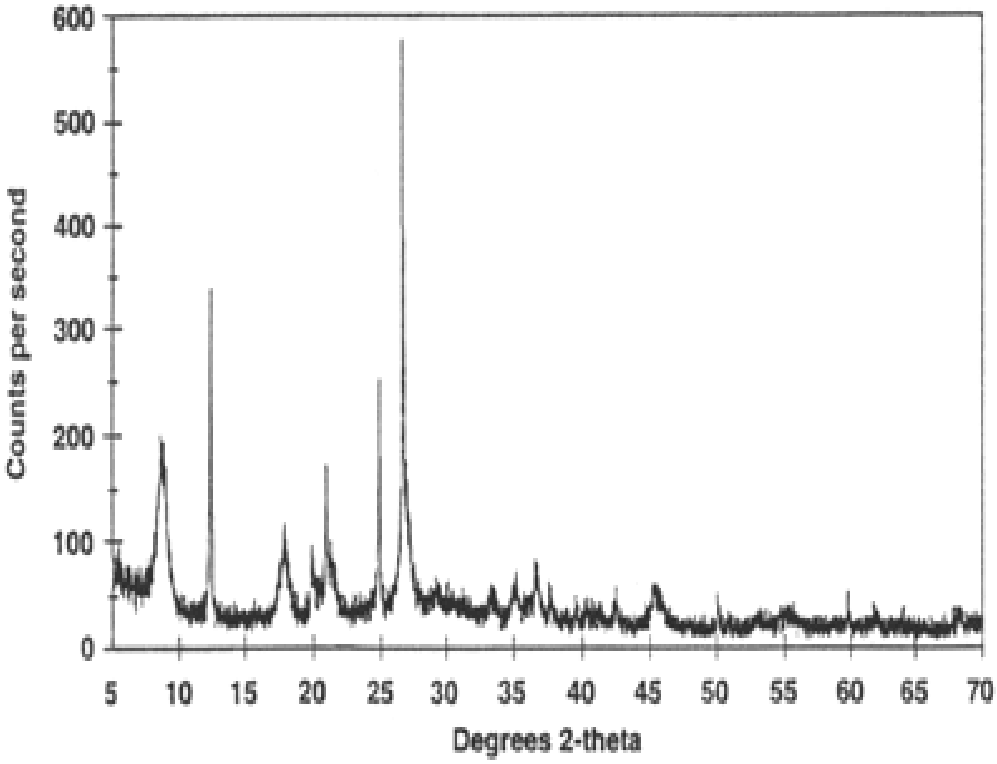

Figure 2.5: X-ray powder diffractogram

The geometry of an X-ray diffractometer is such that the sample rotates in the path of the collimated X-ray beam at an angle θ while the X-ray detector is mounted on an arm to collect the diffracted X-rays and rotates at an angle of 2θ. The instrument used to maintain the angle and rotate the sample is termed a goniometer. For typical powder patterns, data is collected at 2θ from 5° to 70°, angles that are preset in the X-ray scan.

2.2.2 Energy Dispersive X-ray Spectroscopy (EDX)

Energy dispersive X-ray spectroscopy (EDS, EDX or EDXRF) is an analytical technique used for the elemental analysis or chemical characterization of a sample. As a type of spectroscopy, it relies on the investigation of a sample through interactions between electromagnetic radiation and matter, analyzing X-rays emitted by the matter in response to being hit with charged particles [46]. Its characterization capabilities are due in large part to the fundamental principle that each element has a unique atomic structure allowing X-rays that are characteristic of an element's atomic structure to be identified uniquely from each other.

To stimulate the emission of characteristic X-rays from a specimen, a high energy beam of charged particles such as electrons or protons or a beam of X-rays, is focused into the sample being studied. At rest, an atom within the sample contains ground state (or unexcited) electrons in discrete energy levels or electron shells bound to the nucleus. The incident beam may excite an electron in an inner shell, ejecting it from the shell while creating an electron hole where the electron was. An electron from an outer, higher-energy shell then fills the hole, and the difference in energy between the higher-energy shell and the lower energy shell may be released in the form of an X-ray.

The number and energy of the X-rays emitted from a specimen can be measured by an energy dispersive spectrometer. As the energy of the X-rays is characteristic of the difference in energy between the two shells, and of the atomic structure of the element from which they were emitted, this allows the elemental composition of the specimen to be measured. The amount of energy released by the transferring electron depends on which shell it is transferring from, as well as which shell it is transferring to.

Furthermore, the atom of every element releases X-rays with unique amounts of energy during the transferring process. Thus, by measuring the amounts of energy present in the X-rays being released by a specimen during electron beam bombardment, the identity of the atom from which the X-ray was emitted can be established.

There are four primary components of the EDS setup: the beam source; the X-ray detector; the pulse processor; and the analyzer. A number of free-standing EDS systems exist. However, EDS systems are most commonly found on scanning electron microscopes (SEM-EDX) and electron microprobes. Scanning electron microscopes are equipped with a cathode and magnetic lenses to

create and focus a beam of electrons. A detector is used to convert X-ray energy into voltage signals; this information is sent to a pulse processor, which measures the signals and passes them onto an analyzer for data display and analysis.

Figure 2.6: The SEM EDX Integrated system

This technique is used in conjunction with SEM and is not a surface science technique. An electron beam strikes the surface of a conducting sample. The energy of the beam is typically in the range 10-20 keV. This causes X-rays to be emitted from the point the material. The energy of the X-rays emitted depends on the material under examination. The X-rays are generated in a region about 2 microns in depth, and thus EDX is not a surface science technique [47]. Due to the low X-ray intensity, images usually take a number of hours to acquire. Elements of low atomic number are difficult to detect by EDX.

The output of an EDX analysis is an EDX spectrum. The EDX spectrum is just a plot of how frequently an X-ray is received for each energy level. An EDX spectrum normally displays peaks corresponding to the energy levels for which the most X-rays had been received. Each of

these peaks is unique to an atom, and therefore corresponds to a single element. The higher a peak in a spectrum, the more concentrated the element is in the specimen.

An EDX spectrum plot not only identifies the element corresponding to each of its peaks, but the type of X-ray to which it corresponds as well. For example, a peak corresponding to the amount of energy possessed by X-rays emitted by an electron in the L-shell going down to the K-shell is identified as a K-Alpha peak. The peak corresponding to X-rays emitted by M-shell electrons going to the K-shell is identified as a K-Beta peak. See Figure 2.14.

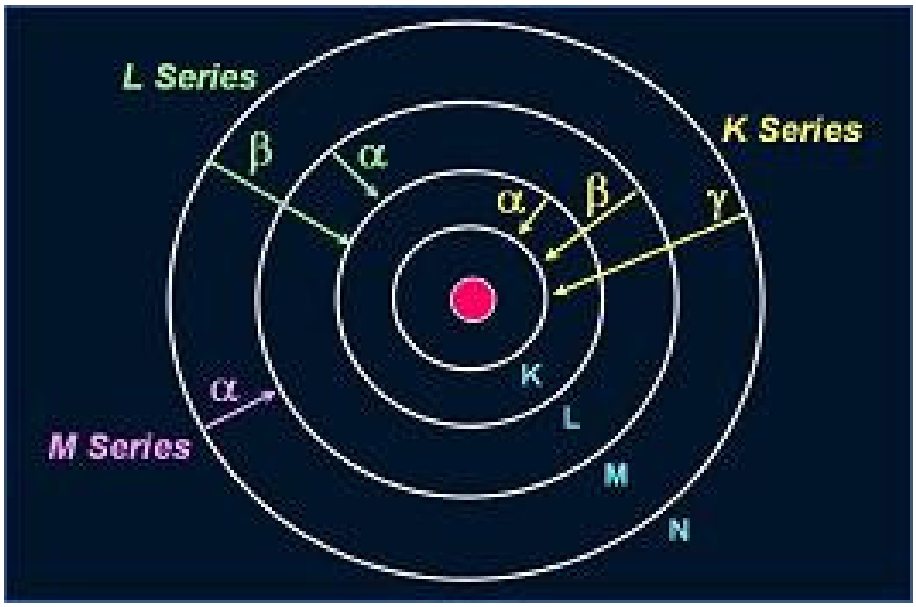

Figure 2.7: Elements in an EDX spectrum are identified based on the energy content of the X-rays emitted by their electrons as these electrons transfer from a higher-energy shell to a lower-energy one.

The most significant issue to note from this is that the X-rays generated from any particular element are characteristic of that element, and as such, can be used to identify which elements are actually present under the electron probe. This is achieved by constructing an index of X-rays collected from a particular spot on the specimen surface, which is known as a spectrum.

2.2.3 Fourier Transform Infrared (FTIR) Spectroscopy

Fourier Transform Infrared (FTIR) spectroscopy is a powerful tool for identifying types of chemical bonds in a molecule by producing an infrared absorption spectrum that is like a molecular "fingerprint". It can be utilized to quantitate some components of an unknown mixture. It can be applied to the analysis of solids, liquids, and gasses [48]. The wavelength of light absorbed is characteristic of the chemical bond as can be seen from the spectrum. By interpreting the infrared absorption spectrum, the chemical bonds in a molecule can be determined. FTIR spectroscopy does not require a vacuum, since neither oxygen nor nitrogen absorbs infrared rays.

Molecular bonds vibrate at various frequencies depending on the elements and the type of bonds. For any given bond, there are several specific frequencies at which it can vibrate. According to quantum mechanics, these frequencies correspond to the ground state (lowest frequency) and several excited states (higher frequencies). One way to cause the frequency of a molecular vibration to increase is to excite the bond by having it absorb light energy. For any given transition between two states the light energy (determined by the wavelength) must exactly equal the difference in the energy between the two states [usually ground state (E_0) and the first excited state (E_1) [49]. The energy corresponding to these transitions between molecular vibrational states is generally 1-10 kilocalorie/mole which corresponds to the infrared portion of the electromagnetic spectrum.

FTIR can provide following information:

• It can identify unknown materials.

• It can determine the quality or consistency of a sample.

• It can determine the amount of components in a mixture.

FTIR spectroscopy was developed in order to overcome the limitations encountered with dispersive instruments. The main difficulty was the slow scanning process. A method for measuring all of the infrared frequencies simultaneously, rather than individually, was needed.

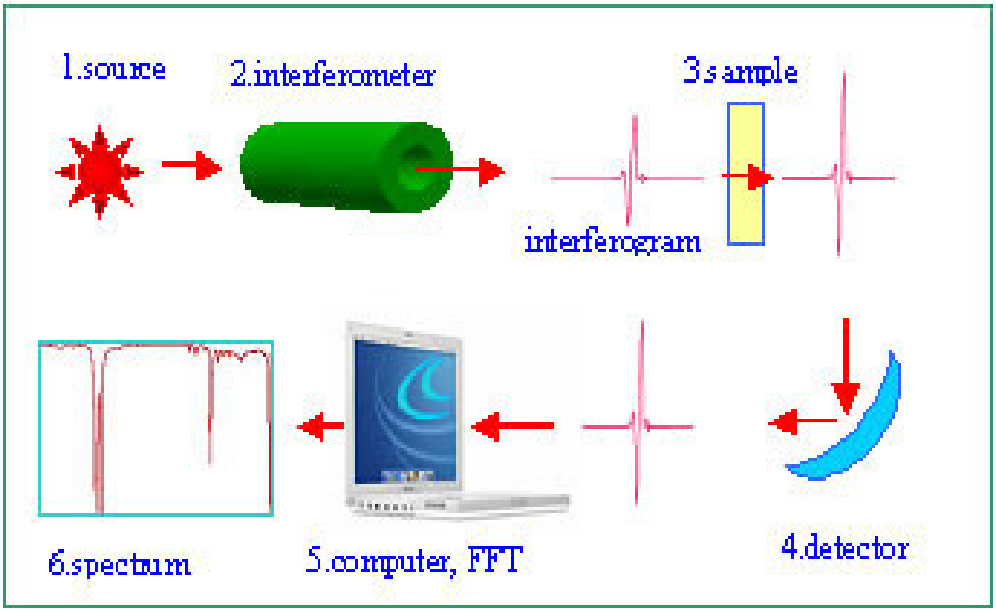

Figure 2.8: Schematic illustration of FTIR system

A solution was developed which employed a very simple optical device called an interferometer. The interferometer produces a unique type of signal which has all of the infrared frequencies "encoded" into it. The signal can be measured very quickly, usually on the order of one second or so. Thus, the time element per sample is reduced to a matter of a few seconds rather than several minutes. Most interferometers employ a beam splitter which takes the incoming infrared beam and divides it into two optical beams. One beam reflects off of a flat mirror which is fixed in place. The other beam reflects off of a flat mirror which is on a mechanism which allows this mirror to move a very short distance away from the beam splitter. The two beams reflect off of their respective mirrors and are recombined when they meet back at the beam splitter. Because the path that one beam travels is a fixed length and the other is constantly changing as its mirror moves, the signal which exits the interferometer is the result of these two beams "interfering" with each other. The resulting signal is called an interferogram which has the unique property that every data point (a function of the moving mirror position) which makes up the signal has information about every infrared frequency which comes from the source.

This means that as the interferogram is measured; all frequencies are being measured simultaneously. Thus, the use of the interferometer results in extremely fast measurements.

Because the analyst requires a frequency spectrum (a plot of the intensity at each individual frequency) in order to make identification, the measured interferogram signal cannot be interpreted directly. A means of "decoding" the individual frequencies is required. This can be accomplished via a well-known mathematical technique called the Fourier transformation. This transformation is performed by the computer which then presents the user with the desired spectral information for analysis.

2.2.4 UV-Visible Absorption Spectroscopy

UV-visible absorption spectroscopy involves the spectroscopy of photons in the UV-visible region. This means it uses light in the visible, near ultraviolet (UV) and near infrared (NIR) ranges. The absorption in the visible ranges directly affects the color of the chemicals involved. In this region of the electromagnetic spectrum, molecules undergo electronic transitions [50]. This technique is complementary to fluorescence spectroscopy, in that fluorescence deals with transitions from the excited state to the ground state, while absorption measures transitions from the ground state to the excited state.

Absorption of light by solution is one of the oldest and still one of the more useful instrumental methods. The wavelength of light that a compound will absorb is characteristic of its chemical structure. Specific regions of the electromagnetic spectrum are absorbed by exciting specific types of molecular and atomic motion to higher energy levels. Absorption of microwave radiation is generally due to excitation of molecular rotational motion. Infrared absorption is associated with vibrational motions of molecules. Absorption of visible and ultraviolet (UV) radiation is associated with excitation of electrons, in both atoms and molecules, to higher energy states. All molecules will undergo electronic excitation following absorption of light, but for most molecules very high energy radiation (in the vacuum ultraviolet, <200 nm) is required. For molecules containing conjugated electron systems however, light in the UV-visible region is adequate. As the degree of conjugation increases, the spectrum shifts to lower energy.

Figure 2.9: UV-Visible experimental set-up

Beer-Lambert Law: The Beer-Lambert law states that the absorbance of a solution is directly proportional to the concentration of the absorbing species in the solution and the path length. Thus, for a fixed path length, UV/VIS spectroscopy can be used to determine the concentration of the absorber in a solution [51]. It is necessary to know how quickly the absorbance changes with concentration.

The amount of light, I, transmitted through a solution of an absorbing chemical in a transparent solvent can be related to its concentration by Beers Law:

$$- \log I/I_o = A = \varepsilon_\lambda bc \qquad \text{--- (2.2)}$$

where I_0 is the incident light intensity, A is the absorbance, b is the cell path length in cm, c is the solution concentration in moles/liter, and ε_λ is the molar absorptivity, (also referred to as the molar extinction coefficient) which has units of liter/mole/cm Notice that ε_λ is a function of wavelength, and it is the quantity which represents the spectrum of the solution.

A diagram of the components of a typical spectrometer is shown in the following diagram. A beam of light from a visible and/or UV light source (colored red) is separated into its component wavelengths by a prism or diffraction grating. Each monochromatic beam in turn is split into two equal intensity beams by a half-mirrored device. One beam, the sample beam (colored magenta), passes through a small transparent container (cuvette) containing a solution of the compound being studied in a transparent solvent. The other beam, the reference (colored blue), passes through an identical cuvette containing only the solvent. The intensities of these light beams are then measured by electronic detectors and compared. The intensity of the reference beam, which should have suffered little or no light absorption, is defined as $\mathbf{I_0}$. The intensity of the sample beam is defined as **I**. Over a short period of time, the spectrometer automatically scans all the component wavelengths in the manner described. The ultraviolet (UV) region scanned is normally from 200 to 400 nm, and the visible portion is from 400 to 800 nm.

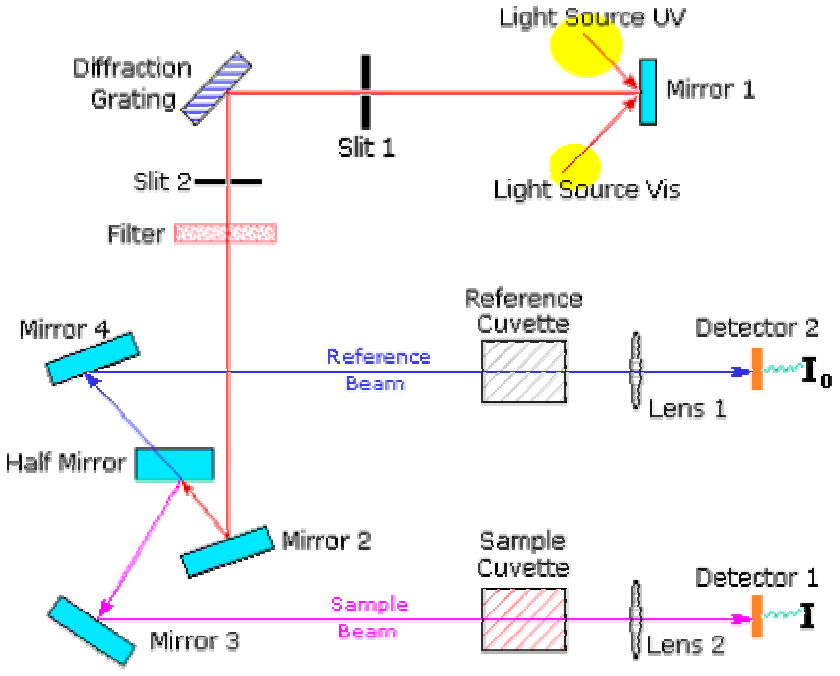

Figure 2.10: Working of UV-Visible spectrometer

2.2.5 Photoluminescence (PL)

2.2.5.1 Introduction to luminescence

Luminescence is the process where an electromagnetic radiation is produced by a substance under suitable external excitation. At certain frequencies, this radiation is significantly in excess of the thermal radiation, which is emitted by a substance at that particular temperature. The so-produced electromagnetic radiation, generally in the visible region, is characteristic of the particular luminescent material under examination, termed as phosphor [52]. The emission of visible light (400-700nm) corresponding to the region between red and violet requires excitation energies the minimum of which is given by Einstein's law stating that the energy,

$$\mathbf{E = h\nu = hc/\lambda} \qquad \textbf{--- (2.3)}$$

If the emission energy is less than the excitation energy, the emission is known as 'Stokes emission', and, if the emission energy is greater than the excitation energy, the emission is known as 'Anti-Stokes' emission. Generally Stokes emission is observed because the difference in energy is caused by the transformation of the exciting light, to a greater or lesser extent, to non-radiating vibration energy of atoms or ions.

Luminescence is further subdivided into fluorescence and phosphorescence [53]. A molecule in an excited state radiates energy after remaining in a metastable state for a fairly long time; the process is termed as **phosphorescence**. The luminescence process in which the molecule emits radiation as it falls directly from an excited state to a lower energy state is known as **fluorescence**. The time scale of the process is of the order of 10^{-8} s. Fluorescence radiation is due to allowed transitions ($\Delta S = 0$) from singlet excited state to the singlet ground state.

If a molecule in an excited state radiates energy after remaining in a metastable state for a fairly long time, the process is termed as phosphorescence. The time scale of the phosphorescence process depends on the energy spacing between the metastable state and the nearest energy state to which transition is allowed and may be of the order of 10^{-6} seconds to minutes, hours or even days. This type of transition is due to forbidden transition ($\Delta S \neq 0$) from the excited metastable state to the lower ground state.

2.2.5.2 Origin of Fluorescence and Phosphorescence

The absorption of energy by a molecule raises it to an excited state. This excited state may be rotational, vibrational or electronic, depending upon the energy of exciting photon. If the energy of the exciting photon is of the order of 10^{-3} eV the rotational states can be excited, if the energy is of the order of 0.1 eV then vibrational states can be excited, and if the energy is of the order of several electron volts then electronic states can be excited. The corresponding spectra are in microwave for rotational, infrared for vibrational and visible as well as ultraviolet range for electronic energy states [54].

A molecule in an excited electronic state can loose energy and return to its ground state in a number of ways. The molecule may come to the ground state by the emission of a photon of same energy in a single step. Another possibility is that it may loose some of its vibrational energy in collision with other molecules. Therefore downward radiative transition originates from a lower vibrational level in the upper electronic state. This phenomenon is called fluorescence and the fluorescent radiation is always of lower frequency Figure 2.11(a).

In molecular spectra, radiative transitions between electronic states of different total spin are prohibited (spin selection rule $\Delta S = 0$). Fig. 2.11(b) shows a situation in which a molecule in its singlet (total spin quantum no. $\Delta S = 0$) ground state, absorbs a photon and is raised to singlet excited state. In collisions the molecule can undergo nonradiative transitions to a lower vibrational level. Now, lower vibrational level may have the same energy as one of the triplet (S=1) excited state. There is then a certain probability of the molecule for a shift to occur to a triplet state. Further collisions in the triplet state bring the molecule's energy below that of the crossover point, so that it is now trapped in the triplet state and ultimately reaches v = 0 level.

As the radiative transition from a triplet to a singlet state is forbidden (_$\Delta S \neq 1$) by spin selection rule, which means not that it is impossible but that it has only a small possibility of occurring. Such transitions have long lifetimes, and the resulting phosphorescent radiation may be emitted in the time interval of the order of seconds, minutes or even hours after the initial excitation is switched off.

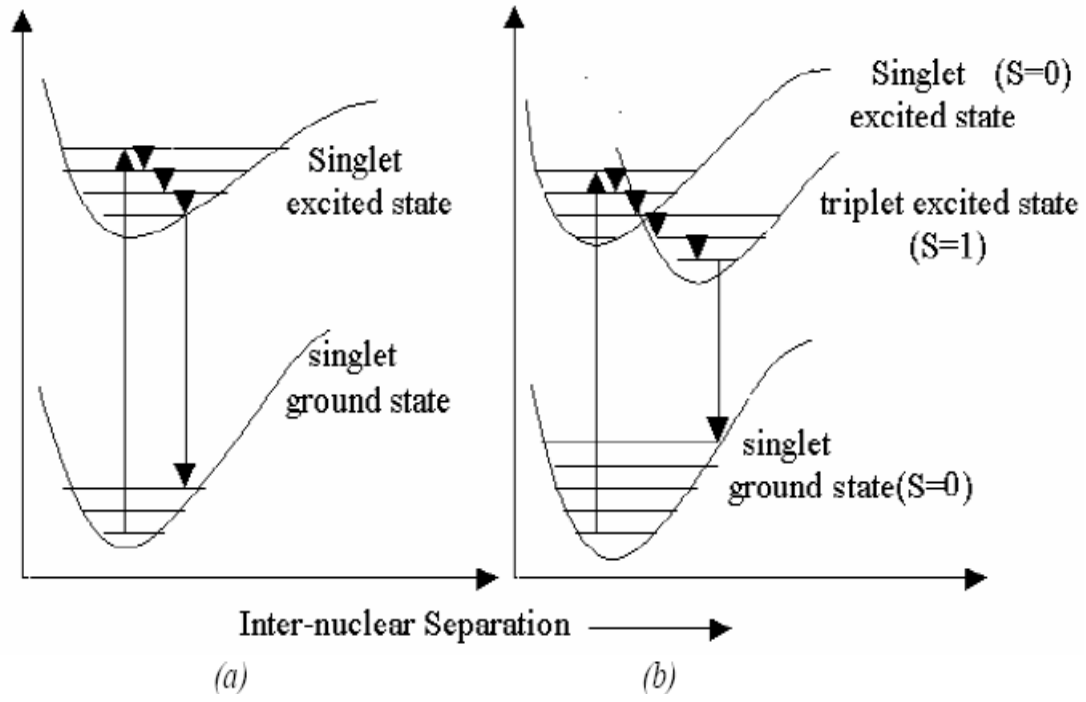

Figure 2.11: (a) origin of fluorescence **(b)** origin of phosphorescence

Depending on how the phosphor is excited, there are several types of luminescence processes and here we discuss Photoluminescence.

Photoluminescence (PL) is a process in which a substance absorbs photons (electromagnetic radiation) and then re-radiates photons [55]. Quantum mechanically, this can be described as an excitation to a higher energy state and then a return to a lower energy state accompanied by the emission of a photon. This is one of many forms of luminescence (light emission) and is distinguished by photo-excitation (excitation by photons), hence the prefix photo-. The period between absorption and emission is typically extremely short, in the order of 10 nanoseconds. Under special circumstances, however, this period can be extended into minutes or hours.

The PL spectrum provides the transition energies, which can be used to determine electronic energy levels. The PL intensity gives a measure of the relative rates of radiative and nonradiative recombination. Variation of the PL intensity with external parameters like temperature and

applied voltage can be used to characterize further the underlying electronic states and bands [56]. PL is simple, versatile, and nondestructive. The instrumentation that is required for ordinary PL work is modest: an optical source and an optical power meter or spectrophotometer. A typical PL set-up is shown in Figure 2.12.

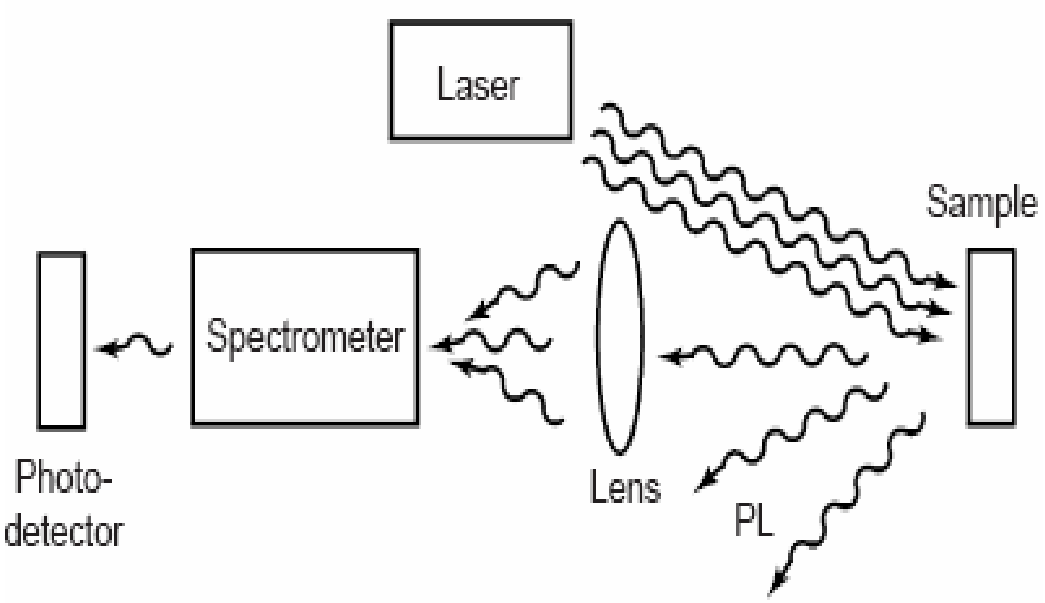

Figure 2.12: Typical experimental set-up for PL measurements

2.2.5.3 Information from PL

Band Gap Determination

The most common radiative transition in semiconductors is between states in the conduction and valence bands, with the energy difference being known as the band gap. Band gap determination is particularly useful when working with new compound semiconductors.

Impurity Levels and Defect Detection

Radiative transitions in semiconductors also involve localized defect levels. The photoluminescence energy associated with these levels can be used to identify specific defects,

and the amount of photoluminescence can be used to determine their concentration.

Recombination Mechanisms

The return to equilibrium, also known as "recombination," can involve both radiative and nonradiative processes. The amount of photoluminescence and its dependence on the level of photo-excitation and temperature are directly related to the dominant recombination process. Analysis of photoluminescence helps to understand the underlying physics of the recombination mechanism.

Material Quality

In general, nonradiative processes are associated with localized defect levels, whose presence is detrimental to material quality and subsequent device performance. Thus, material quality can be measured by quantifying the amount of radiative recombination.

CHAPTER 3

METHODS OF PREPARATION & SYNTHESIS

3.1 Methods of Preparation

During the last one decade, a number of synthesis methods have been reported for the preparation of various intrinsic semiconductor nanocrystals and the method of preparation for doped nanoparticles are still evolving. Generally the doping of bulk semiconductors is carried out by high temperature thermal diffusion or molecular deposition techniques including chemical vapor deposition, atomic layer epitaxy, gas phase deposition, vacuum evaporation, etc. In case of nanoparticles, the incorporation of impurities into quantum-confined systems, containing only few tens of atoms or molecules is much more difficult and complex because no conventional high temperature processes can be applied. In this case, doping has to be carried out by low temperature processes, mostly by wet-chemical synthetic routes like chemical precipitation. The doping through wet-chemistry invites some new difficulties that are not encountered in the case of bulk material. For example, the dopant ions used in the reaction may preferably precipitate, as a stable phase, prior to the incorporation into the host lattice leading to very low or no doping at all. Further, even though dopant ions are incorporated into the lattice, these may tend to diffuse on to the nanoparticles surface or the surrounding matrix because the impurity ions are always only a few lattice constant away from the surface. Thus the preparation of effectively doped semiconductor nanocrystals and their application in the nanotechnology frontier still remain a challenging task.

3.2 Synthesis of doped ZnS Nanoparticles

ZnS nanoparticles have been prepared by chemical precipitation method at room temperature. The chemical precipitation technique has been found to have a number of advantages including easy process ability at ambient conditions , possibility of doping of different kinds of impurities with high doping concentration even at room temperature, good control over the chemistry of doping, easiness of surface capping with a variety of different steps involved in the synthesis process of nanoparticles.

Doped ZnS:Eu nanoparticles were precipitated from a mixture of zinc acetate and europium trichloride with sodium sulfide in aqueous solution. In a typical procedure, aqueous solution of sodium sulfide was added into aqueous solution of zinc acetate and aqueous solution of europium trichloride with the molar ratio of Zn:S being 1:1 to obtain white fluid. The different concentrations of Eu taken are as follows: 1mM, 1.5mM, 2mM, 2.5mM, 3mM, 4mM, and 5mM.Then mercaptoethanol ($HOCH_2CH_2SH$) was added to the above solution, with constant stirring at room temperature. The resulting precipitates were filtered and washed several times with double distilled water and ethanol. Washings were done to remove any organic part or any other impurities from the particles.

The product in the form of thick paste was dried in vacuum at 60 ^{o}C for around a day. In addition, undoped ZnS nanoparticles were also synthesized in the same conditions, but without the addition of dopants.

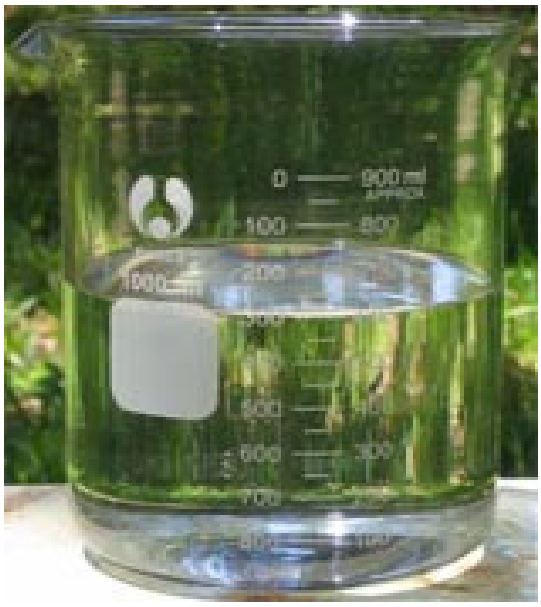

Figure 3.1: Clear solution formed after stirring

Figure 3.2: Solution on Magnetic Stirrer

Figure 3.3: White solution of ZnS:Eu nanoparticles

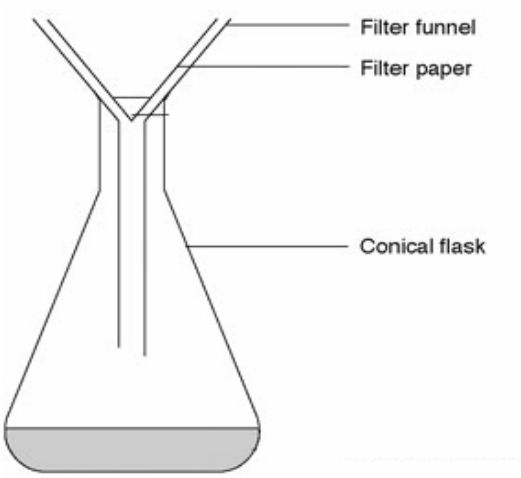

Figure 3.4: Filtration of particles

3.3 Heat Treatment

Heat treatment is the process of heating the sample to a predetermined temperature, holding for a certain time, and then cooling to room temperature to improve its properties. Heat treatment is a method used to alter the physical, and chemical, properties of a material.

Since heat treatment in air is known to cause oxidation of ZnS, the as-synthesized nanoparticles were heated at temperature 200^{o}C in oven under nitrogen atmosphere as shown in figure 3.5 for two hours and then allowed to cool inside the oven upto room temperature.

Figure 3.5: Oven for heat treatment of the nanoparticles

\

Different samples were prepared by varying the concentration of Europium and the samples were named as shown in table below:

Table 3.1: Names given to different samples

S. No.	Sample	Sample Name (as synthesized)	Sample Name (After heat treatment)
1	ZnS	Eu0	Eu0 H
2	ZnS:Eu (1mM Eu)	Eu1	Eu1 H
3	ZnS:Eu (1.5mM Eu)	Eu1.5	Eu1.5 H
4	ZnS:Eu (2mM Eu)	Eu2	Eu2 H
5	ZnS:Eu (2.5mM Eu)	Eu2.5	Eu2.5 H
6	ZnS:Eu (3mM Eu)	Eu3	Eu3 H
7	ZnS:Eu (4mM Eu)	Eu4	Eu4 H
8	ZnS:Eu (5mM Eu)	Eu5	Eu5 H

Chapter 4

RESULTS AND DISCUSSION

4.1 X-Ray Diffraction Studies

XRD studies are an efficient tool for analyzing the structural properties of the sample. In the present studies, XRD pattern have been recorded using X'PERT PRO Panalytical powder X-ray diffractometer using characteristic wavelength of 1.5418 Å. The XRD pattern of as-synthesized and heat treated (at 200 ^{o}C for 2 hours in nitrogen gas atmosphere) samples of ZnS, doped with Eu (1 and 4 mM), are shown, respectively in the figure 4.1 and 4.2. Comparison of the recorded XRD pattern with standard JCPDS data file 05-0566 confirms the cubic crystal structure. As seen from figures 4.1 and 4.2, the diffraction peaks from (111), (220), and (311) planes have only appeared in the XRD pattern and all other high-angle peaks have submerged in the background due to the large line broadening, which is attributed to nanosize of the particles [57]. Moreover, on heat treatment the diffraction peaks are more intense and sharp. This shows that the heating has increased the crystallanity of the nanoparticles.

Tables 4.1and 4.2, show the comparison between the standard intensity of the diffraction peaks with the observed intensity, of the ZnS:Eu (1 mM and 4 mM) nanoparticles, respectively, with and without heat treatment. The intensity of the diffraction peaks of the heat treated sample matches well with that of the standard data, as compared to the as-synthesized sample.

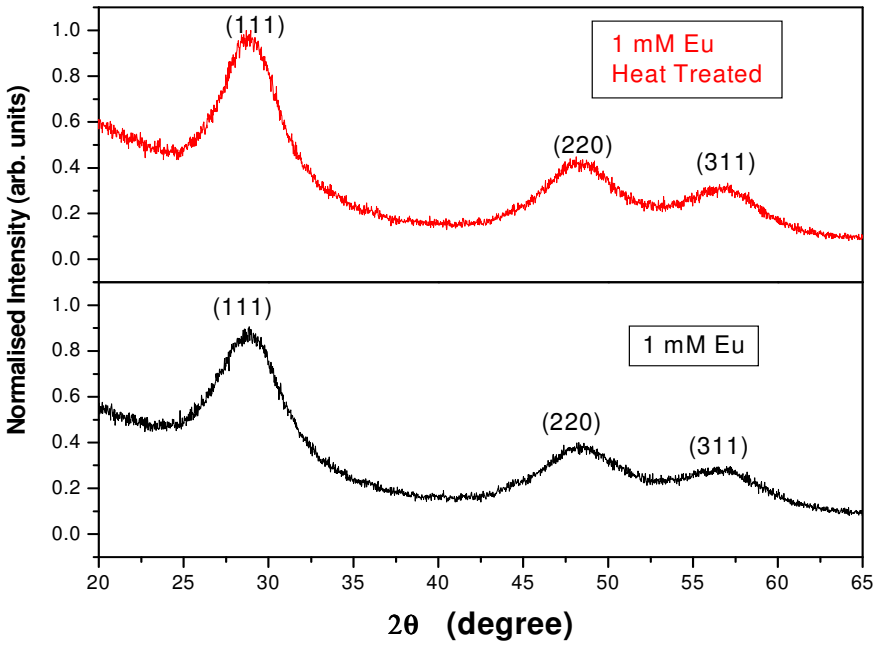

Figure 4.1: X-ray diffraction pattern of ZnS:Eu (1 mM) nanoparticles, with and without heat treatment

Table 4.1: Comparison of intensities of diffraction peaks for ZnS:Eu (1mM) nanoparticles

Observed 2θ (degree)	Standard Intensity	Observed Intensity	Observed Intensity (Heat treated sample)	(hkl)
28.996	100	90.0	99.5	(111)
48.488	51	39.7	44.2	(220)
56.355	30	29.3	32.2	(311)

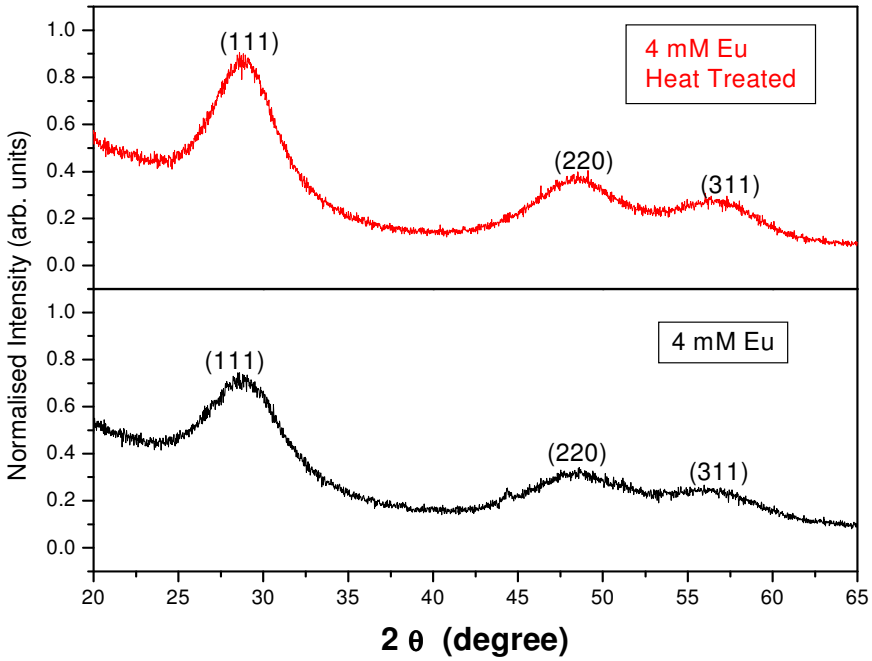

Figure 4.2: X-ray diffraction pattern of ZnS:Eu (4 mM) nanoparticles, with and without heat treatment

Table 4.2: Comparison of intensities of diffraction peaks for ZnS:Eu (4 mM) nanoparticles

Observed 2θ (degrees)	Standard Intensity	Observed Intensity	Observed Intensity (heat treated)	(hkl)
28.888	100	75.9	91.04	(111)
49.244	51	35	40.8	(220)
56.933	30	27.2	29.6	(311)

Average crystallite size has been calculated from the recorded XRD pattern using well known Debye Scherrer Equation [17]:

$$D = 0.94\lambda / B \cos\theta \quad \ldots (4.1)$$

where *D* is the average crystallite size, λ is the wavelength of incident X-ray, *B* is the full width at half maximum (FWHM) of the diffraction peak expressed in radian and θ is the Bragg`s angle. The mean calculated crystallite size of the ZnS:Eu nanoparticles is of the order of Bohr`s Exciton radius for ZnS, 5 nm, which shows that the synthesized nanoparticles are in the quantum confinement regime. Thus, these nanoparticles may also be called the quantum dots. Moreover, it is also seen from table 4.3, that the crystallite size has increased on heat treatment of the samples by a fraction of nm.

Table 4.3: Crystallite sizes of all the ZnS:Eu nanoparticles

Sample Name	Crystallite Size (nm)
ZnS:Eu (1 mM)	4.98
ZnS:Eu (1 mM) Heat Treated	5.34
ZnS:Eu (4 mM)	4.5
ZnS:Eu (4 mM) Heat Treated	4.9

.

4.2 Energy Dispersive X-ray (EDX) Spectroscopy

EDX spectroscopy is an analytical tool to determine the composition of the sample. The composition of the ZnS:Eu (3 mM) nanoparticles was analyzed by EDAX spectroscopy, using Noran System Six, as shown in figure 4.3. Electron beam induced inner-shell ionization and subsequent emission of characteristic fluorescence are analyzed in order to obtain the composition.

As shown in figure 4.3, Zn L-fluorescence (Lα around 1 keV energy range), Zn K-fluorescence (Kα in the energy range 8-9 keV and Kβin the energy range 9-10 keV), S K-fluorescence (Kα in

the 2-3 keV energy range) and Eu L & M-fluorescence (Lα, Lβ and Lγ in the energy range 6-8 keV, and Mα in the energy range 0.5 to 1.5 keV) are observed. Apart from these the Kα fluorescence from carbon and oxygen has also been detected. This fluorescence spectrum shows the presence of Zn, S and Eu as the elementary components.

The atomic ratio of Zn : S : Eu is 1.000 : 0.808 : 0.002. This shows that the incorporation of Eu is quite poor in the ZnS nanoparticles. There are several reasons for the poor incorporation of Eu^{3+} in nanocrystalline ZnS. First, the ionic radius of the Eu^{3+} ion (0.95 Å) is larger than that of Zn^{2+} (0.75 Å). For an Eu^{3+} ion to replace a Zn^{2+} lattice site, the ZnS host lattice has to deform, which is energetically unfavorable. Besides, due to the large ionic radius, the Eu^{3+} ion prefers sites with high coordination numbers (six or higher). In ZnS, however, the coordination number of the cation lattice site is only four, which is very unusual for Eu^{3+}. In addition, the 3+ charge of the Eu^{3+} ion has to be compensated for somewhere in the lattice. It is questionable if Eu can be incorporated in a sulfide in the trivalent state. The divalent state is expected to be more stable. [58].

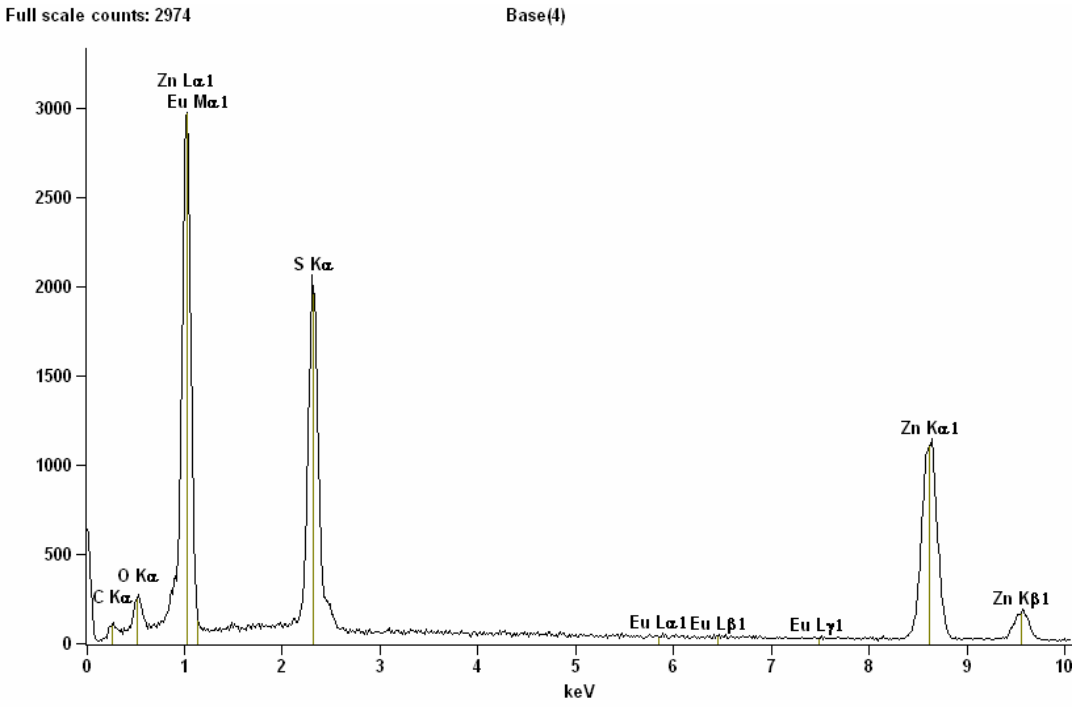

Figure 4.3: EDAX spectrum of the ZnS:Eu (3mM) sample

4.3 Fourier Transform Infrared (FTIR) Spectroscopy

The organic composition of the samples and the presence of various bonds have been studied through Fourier Transform Infra-red Spectroscopy (FTIR). As shown in figure 4.4, the FTIR spectra of ZnS nanoparticles with and without heat treatment show the presence of OH group, with a broad band centered at around 3663 cm^{-1}.

A moderate peak near 1590 cm^{-1} might be due to the presence of carboxylate ion. This peak shows that the acetate group from the zinc acetate precursor used for zinc ions, have been retained in the synthesized nanoparticles. The weak band appearing at 1392 cm^{-1} and 1372 cm^{-1} may be attributed to O-H bending in carboxylic acids. It might be due to O-H in-plane bending vibrations in alcohols. The weak peaks appearing in both, Eu0 and Eu0 heat treated sample, at 1220 cm^{-1} and at 1224 cm^{-1} respectively, might be due to C-O stretching. It may be due to bending vibrations of C-H due to absorption of hydrocarbons. The weak peak appearing in both, Eu0 and Eu0 heat treated sample, at 666 and 670 cm^{-1} respectively might be due to the presence of C-S linkage. This shows the presence of mercaptoethanol ($HOCH_2CH_2SH$), which has been used as the surfactant/capping agent in the synthesis of the ZnS:Eu nanoparticles.

Moreover, no appreciable change has been observed in the FTIR spectra, on increasing the concentration of Eu and on heat treating the synthesized sample. This shows the presence of mercaptoethanal even after the heat treatment.

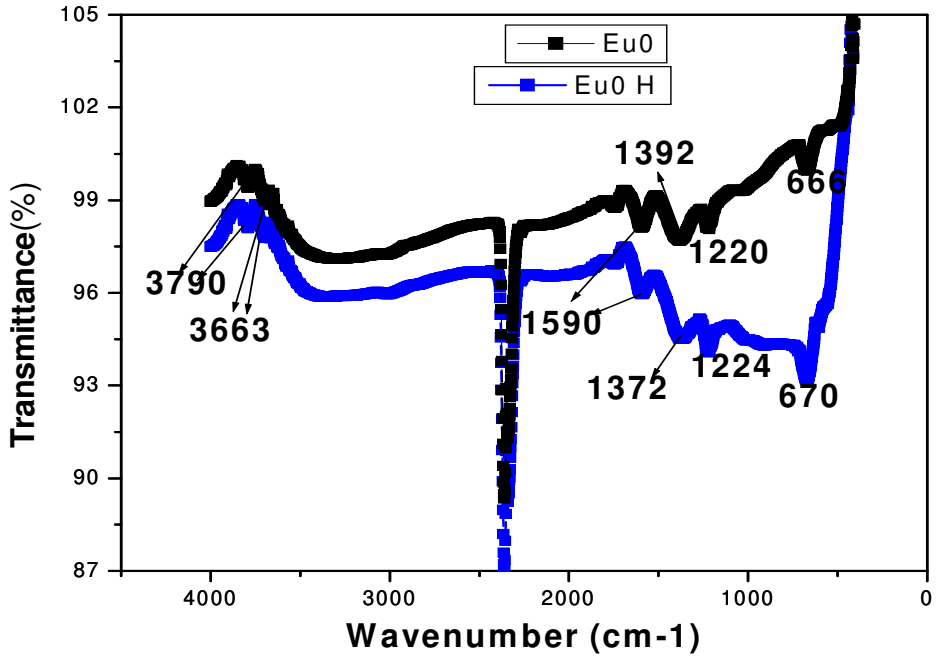

Figure 4.4: FTIR Spectrum of ZnS undoped nanoparticles, with and without heat treatment.

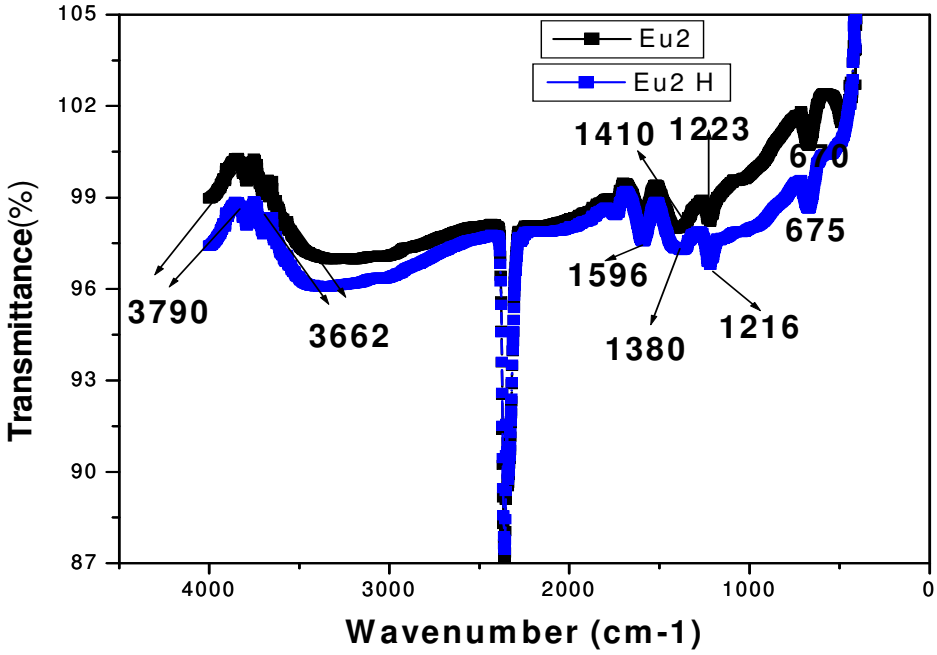

Figure 4.5: FTIR Spectrum of ZnS doped (with Eu 2mM) nanoparticles, with and without heat treatment.

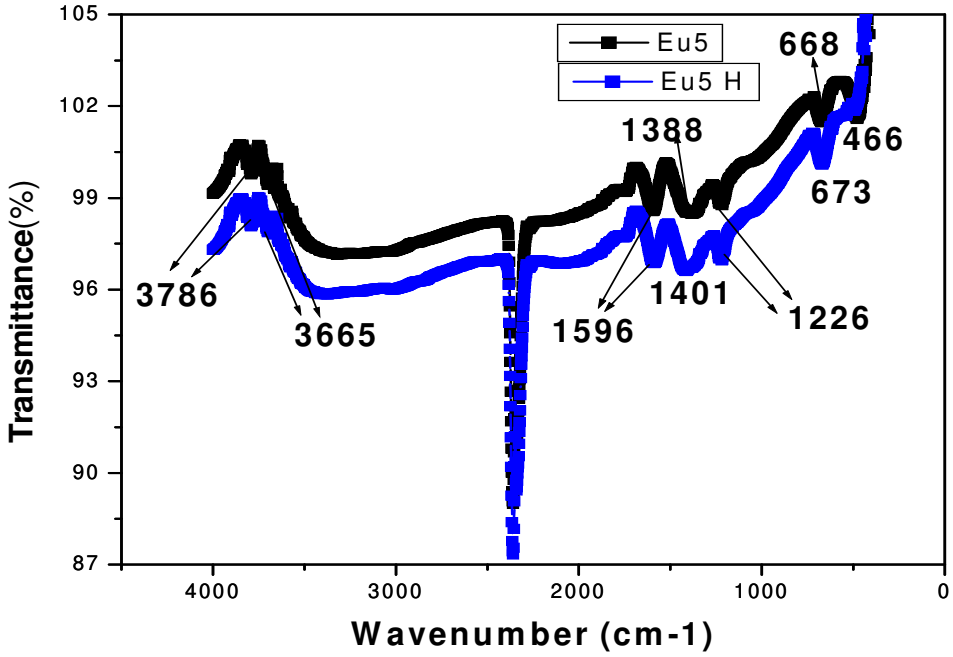

Figure 4.6: FTIR Spectrum of ZnS doped (with Eu 5mM) nanoparticles, with and without heat treatment.

4.4 Optical Characterization

4.4.1 UV-Visible Absorption studies

Undoped and Eu doped ZnS nanoparticles, finely dispersed in ethanol, have been used for the UV- visible absorption studies by using Specord 205 spectrophotometer (Analytik Jena).

Figures 4.7 to 4.12 show the UV-visible absorption spectra of the ZnS:Eu nanoparticles, with and without heat treatment. All the spectra show an absorpion edge around 325 nm, with a slight red shift observed after the heat treatment of the samples. Moreover, the as-synthesized samples show the excitonic peak centered at around 315 nm. This is due to the quantum confinement effect. Whereas, this excitonic peak fades away, after heat treatment. This can also be supported by the increase in crystallite size after heat treatment, as caluculated by Debye's formula in XRD studies.

Moreover, ZnS is a direct band gap semiconductor. Therefore, the optical band gap values have been calculted from the differential minima of the absorbance versus energy plots. Band gap of ZnS:Eu calculated by differential minima varies from 3.8 to 4.6, as shown in table 4.4. This value has been found to be higher than that of the bulk ZnS, 3.67 eV. This enhancement in the optical band gap can be attributed to the quantum cconfinement effects.

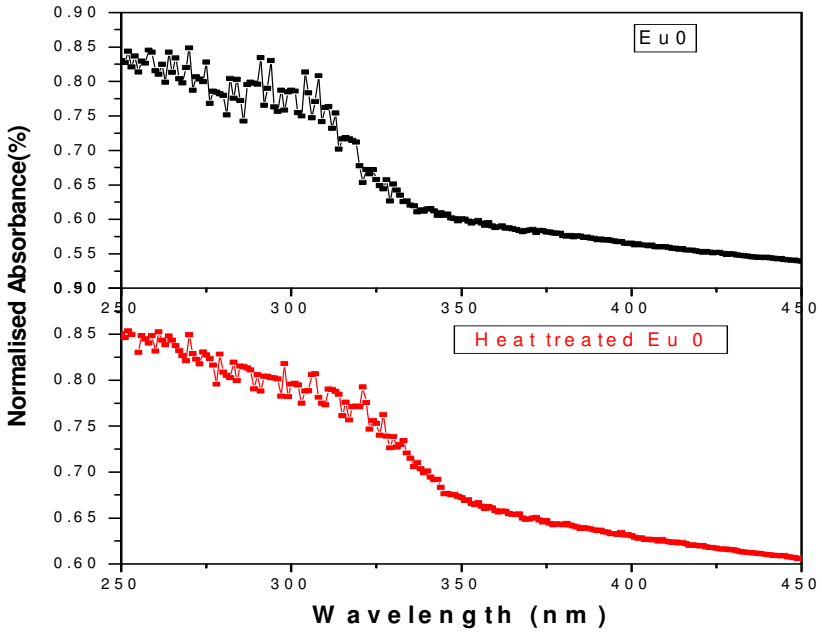

Figure 4.7: Absorbance Vs. wavelength graph of ZnS undoped with and without heat treatment.

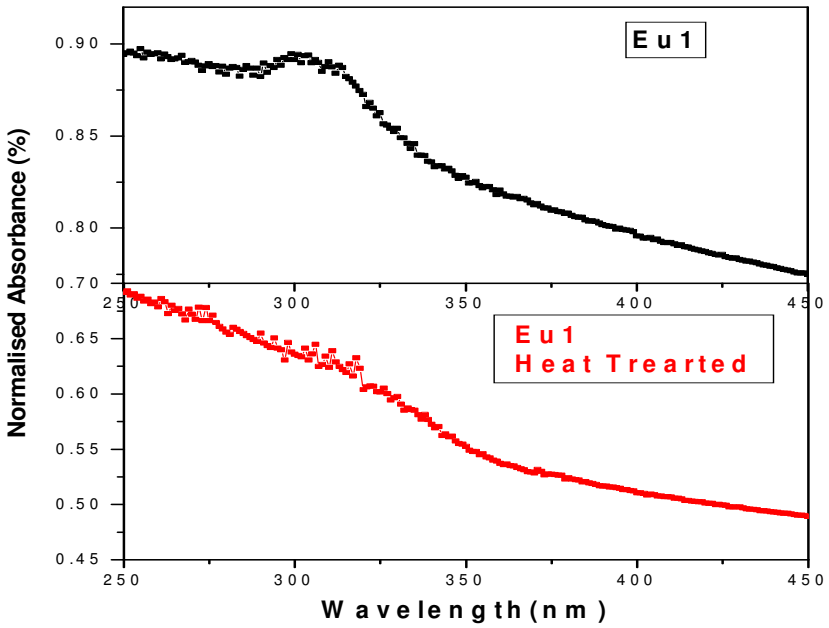

Figure 4.8: Absorbance Vs. wavelength graph of ZnS:Eu (1mM) with and without heat treatment

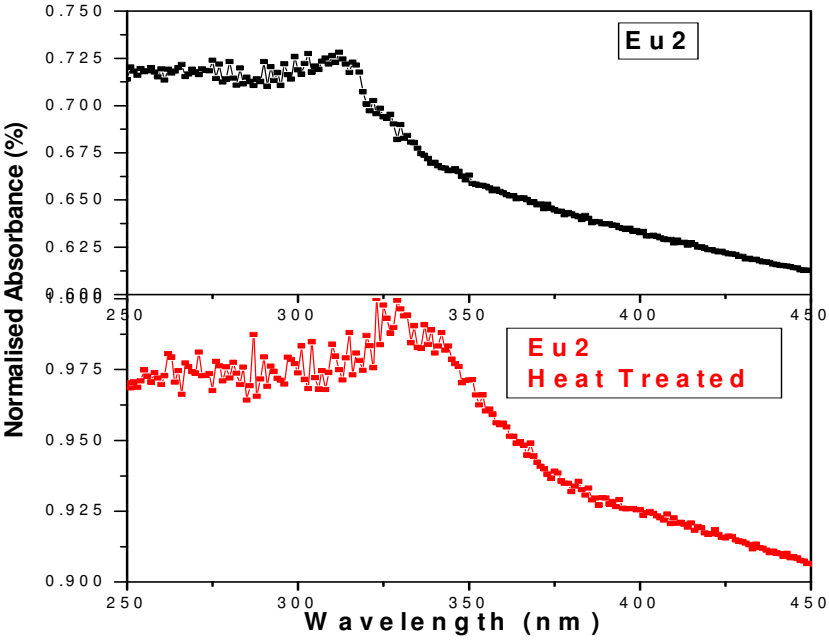

Figure 4.9: Absorbance Vs. wavelength graph of ZnS:Eu (2 mM) with and without heat treatment

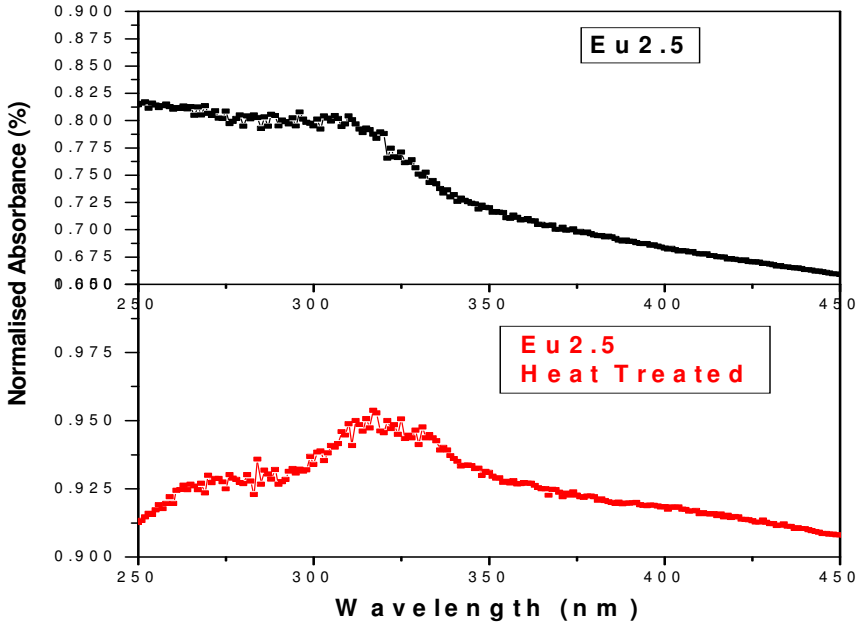

Figure 4.10: Absorbance Vs. wavelength graph of ZnS:Eu (2.5 mM) with and without heat treatment

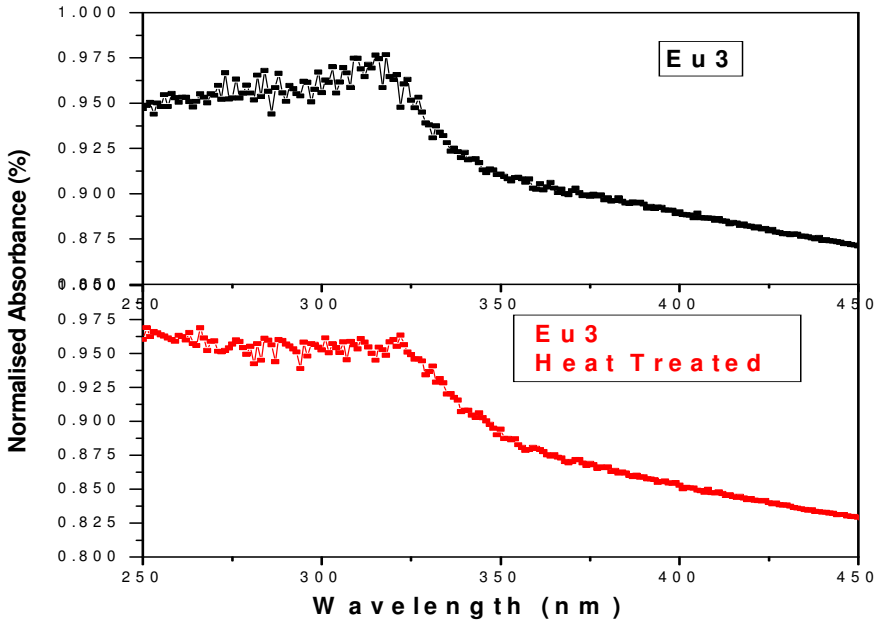

Figure 4.11: Absorbance Vs. wavelength graph of ZnS:Eu (3 mM) with and without heat treatment

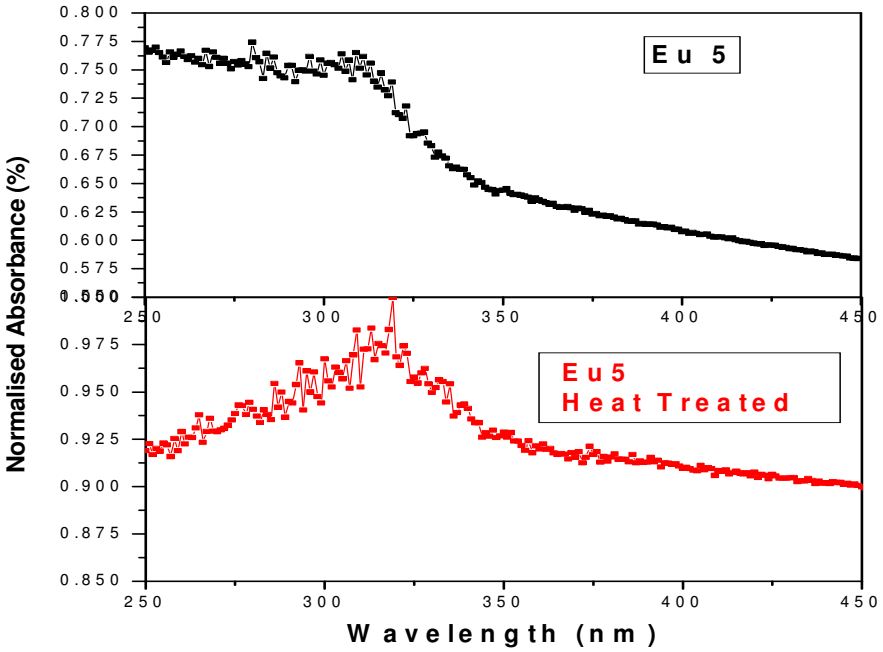

Figure 4.12: Absorbance Vs. wavelength graph of ZnS:Eu (5 mM) with and without heat treatment

Table 4.4: Band gaps of different ZnS:Eu nanoparticles

Sr. No.	Sample Name	Band gap (eV)
1	ZnS:Eu0	4.2
2	ZnS:Eu0 H	3.8
3	ZnS:Eu1	3.9
4	ZnS:Eu1 H	3.9
5	ZnS:Eu1.5	3.7
6	ZnS:Eu1.5 H	3.9
7	ZnS:Eu2	3.9
8	ZnS:Eu2 H	4.1
9	ZnS:Eu2.5	3.9

10	ZnS:Eu2.5 H	3.9
11	ZnS:Eu3	4.3
12	ZnS:Eu3 H	4.6
13	ZnS:Eu4	3.9
14	ZnS:Eu4 H	4.1
15	ZnS:Eu5	3.9
16	ZnS:Eu5 H	3.8

4.4.2 Photoluminescence (PL) Studies

Room temperature PL spectra of the finely dispersed ZnS:Eu nanoparticles have been measured using a xenon lamp source spectrophotometer (Cary Varian), at an excitation wavelength 320 nm.

Figure 4.13 shows the room temperature PL spectra of ZnS undoped and ZnS:Eu nanoparticles. The spectrum for undoped ZnS nanoparticles is broad and asymmetric, whereas on doping the nanoparticles with Eu ions, the spectra have become sharp. This shows that the Eu doping has removed the number of surface defects leading to radiative transitions. The emission at 360 nm (3.4 eV) may be due to the near band edge transitions, which can be supported by the absorption spectra showing the absorption maxima in this range. The emission at 425 and 434 nm has been known due to the recombination between the sulfur-vacancy-related donor and the valence band [59].

In the synthesis process, Eu^{3+} ions have been used. However, the possibility of Eu^{3+} ions to occupy the ZnS lattice is quite less. This may be due to the ionic radius of the Eu^{3+} ion (0.95 Å) being larger than that of Zn^{2+} (0.75 Å). For Eu^{3+} ion to replace a Zn^{2+} lattice site, the ZnS host lattice has to deform, which is energetically unfavorable. Besides, due to the large ionic radius, the Eu^{3+} ion prefers sites with high coordination numbers (six or higher). In ZnS, however, the coordination number of the cation lattice site is only four, which is very unusual for Eu^{3+}. In

addition, the 3+ charge of the Eu^{3+} ion has to be compensated for somewhere in the lattice. It is questionable if Eu can be incorporated in a sulfide in the trivalent state. The divalent state is expected to be more stable [58]. This has also been discussed in EDX from other point of view.

Moreover, as reported by many researchers [26, 29], Eu^{3+} ions in ZnS give PL emission at 590, 612 and 695 nm due to $^5D_0 \rightarrow {}^7F_1$, $^5D_0 \rightarrow {}^7F_2$ and $^5D_0 \rightarrow {}^7F_4$, respectively. But no such emission has been found in our results as shown in figure 4.13.

This shows the possibility of the reduction of Eu ions as follows:

$$\mathbf{Eu^{3+} + e^- \rightarrow Eu^{2+}} \qquad \textbf{…(4.2)}$$

Therefore, the blue emission centered at 485 nm and the green emission peak at 525 nm may be attributed to Eu^{2+} related emission, due to the $4f^7 \rightarrow 4f^6 5d^1$ radiative transitions. This emission discussed here, is not consistent to the red emission in alkaline earth sulphides, because the 5d excited states of Eu^{2+} ion are host sensitive and therefore, the $4f^6 5d^1$ states split due to spin-orbit coupling and crystal field [25], resulting in blue and green emissions. As shown in figures 4.14 to 4.19, the emission intensity has decreased with heat treatment. Whereas there is no shift in the peak position has been observed.

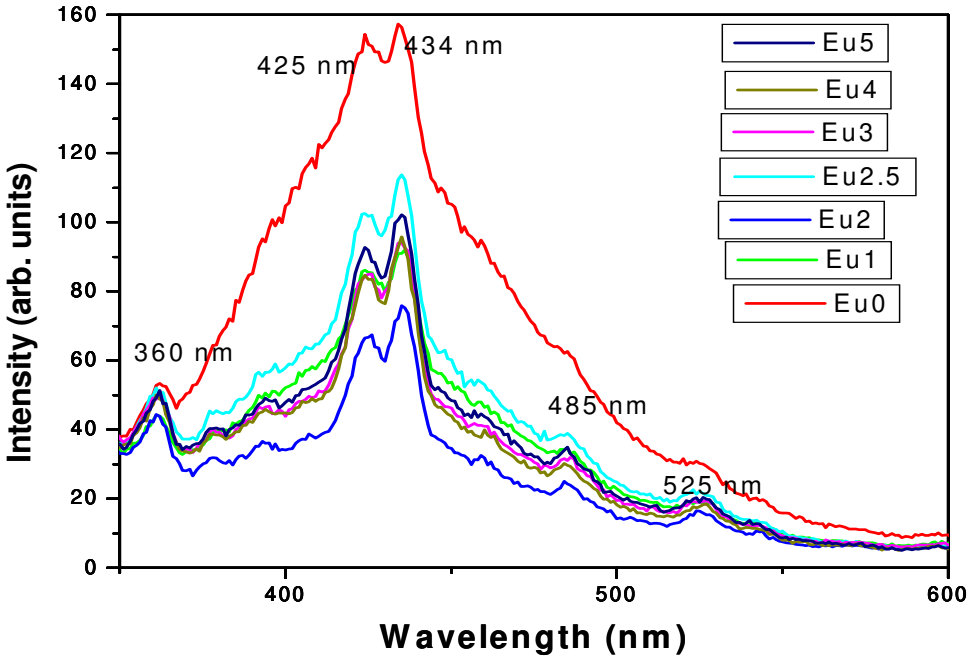

Figure 4.13 Room temperature PL spectra of ZnS:Eu (at different concentrations of Eu) nanoparticles using the excitation wavelength of 320 nm

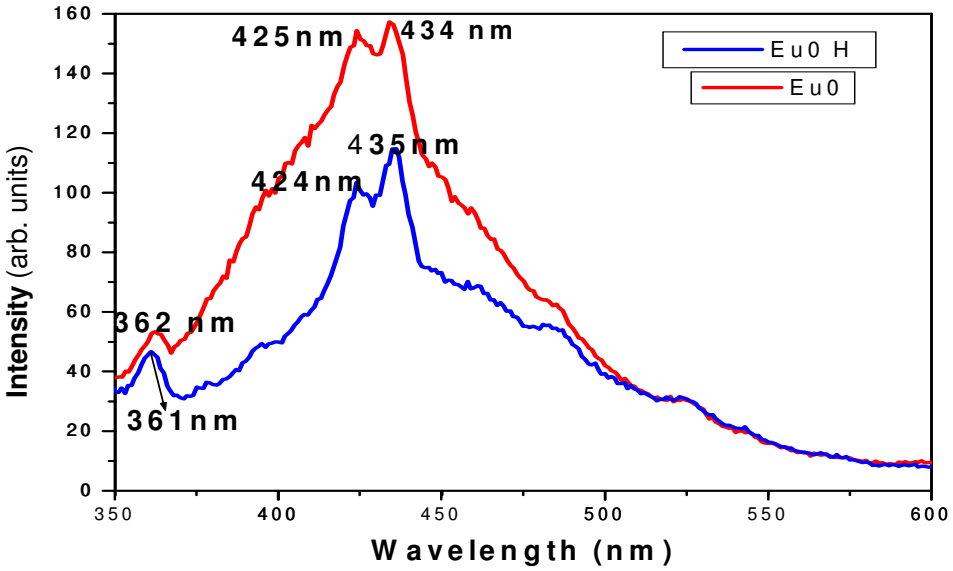

Figure 4.14: Room temperature PL spectra of ZnS nanoparticles, with and without heat treatment using the excitation wavelength of 320 nm

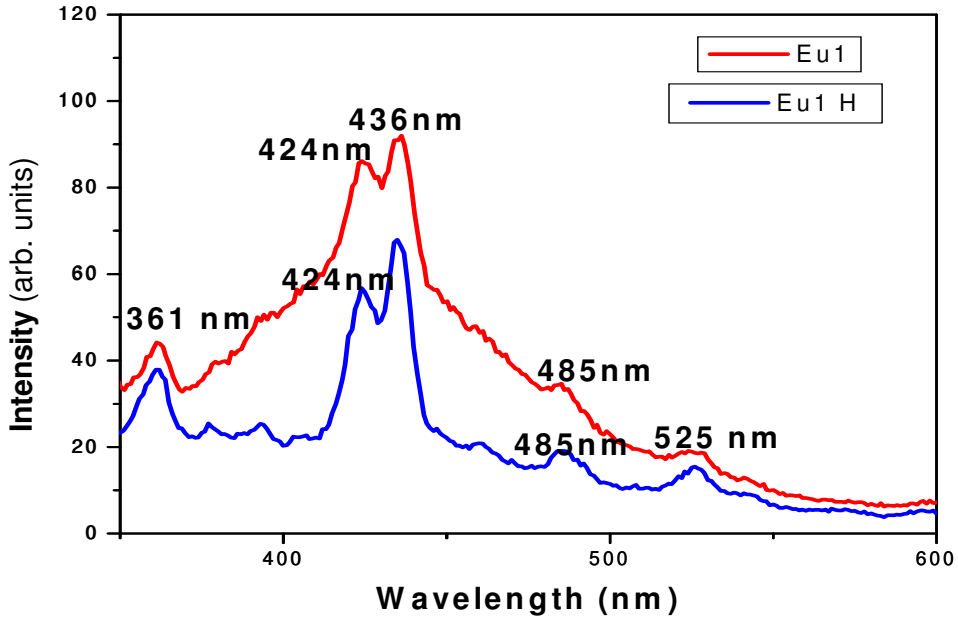

Figure 4.15: Room temperature PL spectra of ZnS:Eu (`1mM) nanoparticles, with and without heat treatment using the excitation wavelength of 320 nm

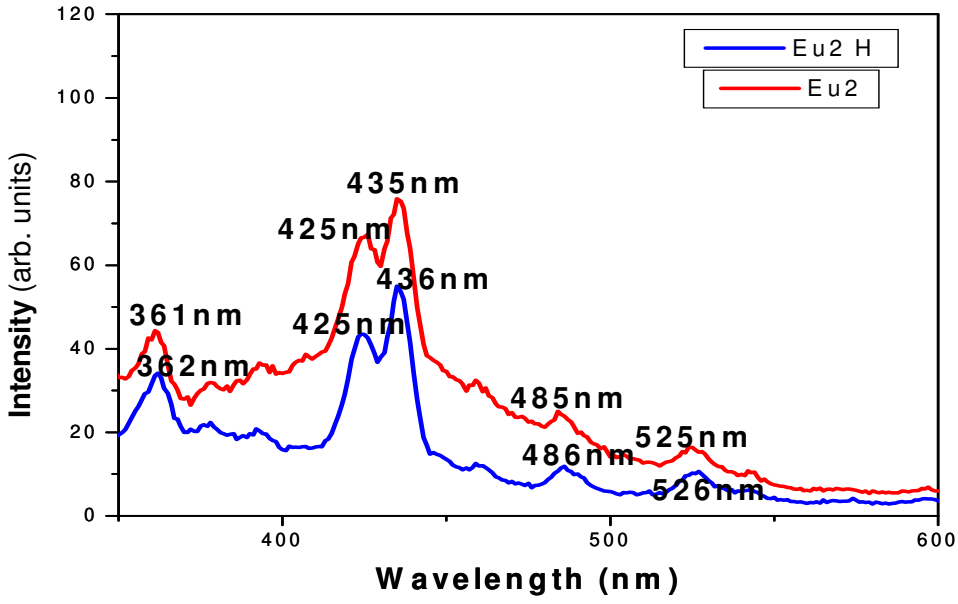

Figure 4.16: Room temperature PL spectra of ZnS:Eu (2mM) nanoparticles, with and without heat treatment using the excitation wavelength of 320 nm

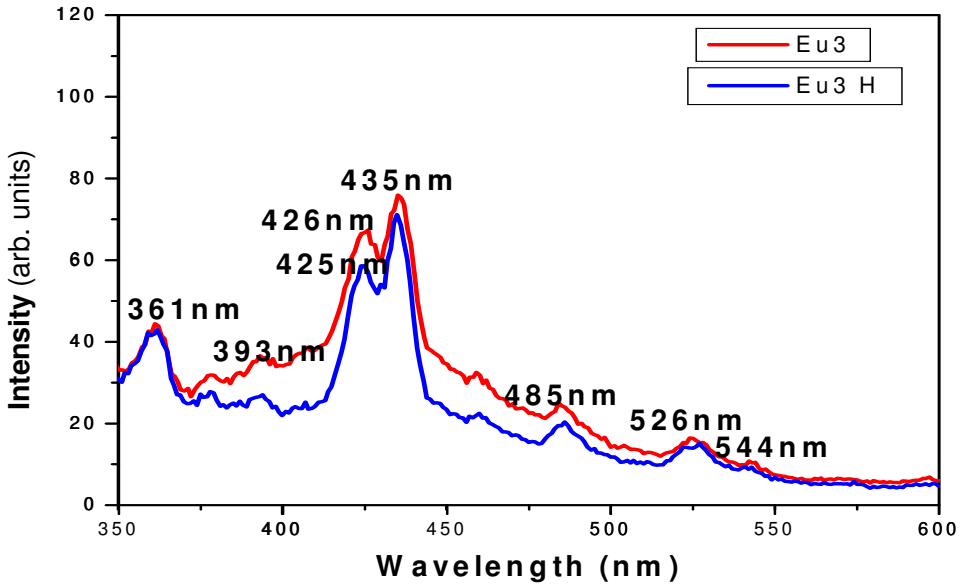

Figure 4.17: Room temperature PL spectra of ZnS:Eu (3mM) nanoparticles, with and without heat treatment using the excitation wavelength of 320 nm

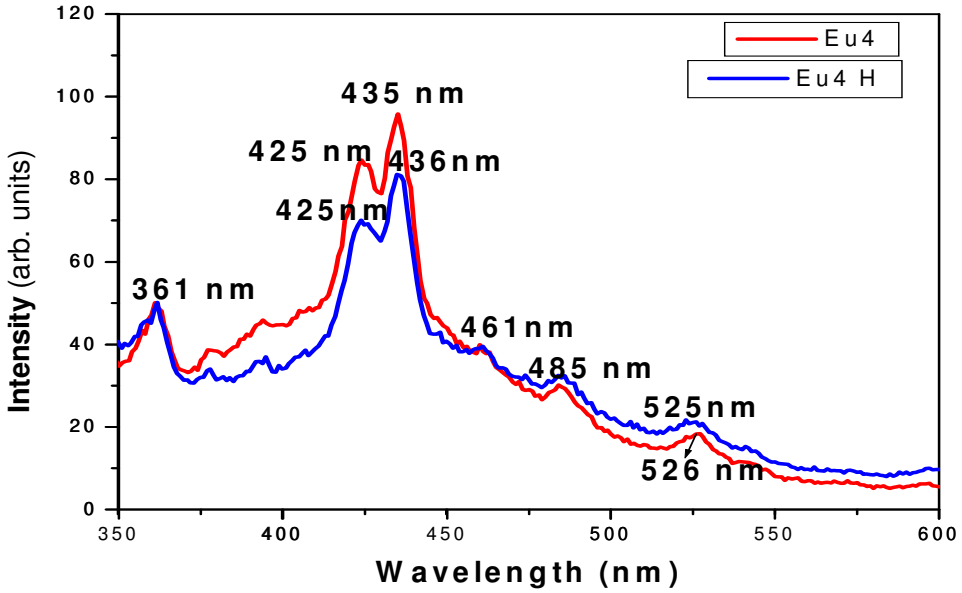

Figure 4.18: Room temperature PL spectra of ZnS:Eu (4mM) nanoparticles, with and without heat treatment using the excitation wavelength of 320 nm

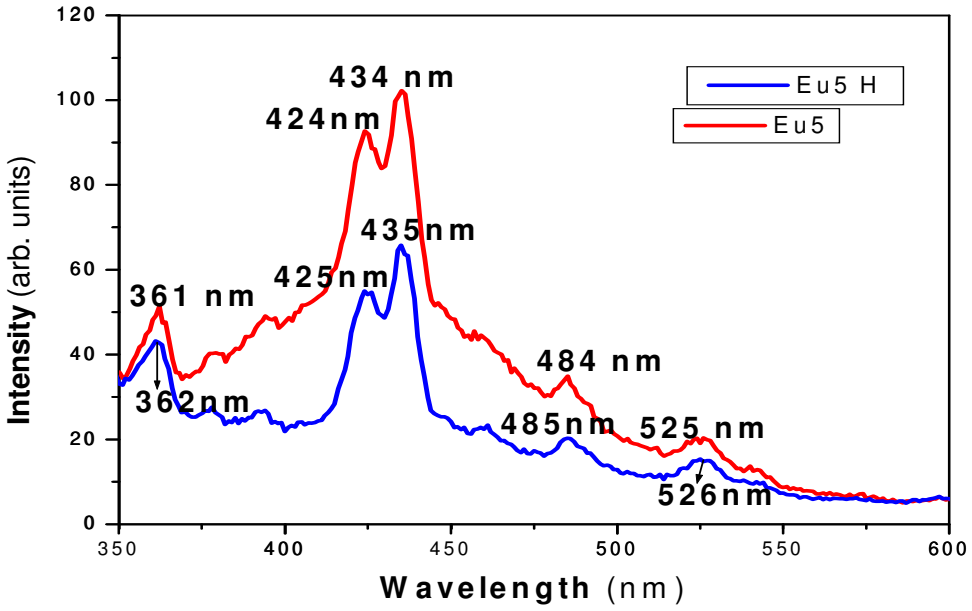

Figure 4.19: Room temperature PL spectra of ZnS:Eu (5mM) nanoparticles, with and without heat treatment using the excitation wavelength of 320 nm

Chapter 5

CONCLUSIONS

Conclusions

The aim of the present work was to investigate the effect of Eu doping and heat treatment on the structural and optical properties of ZnS nanoparticles. The synthesis of ZnS:Eu nanoparticles has been carried out by chemical precipitation method, with water as a solvent, and at room temperature. The samples have been heat treated at 200 ^{o}C for 2 hours in nitrogen gas atmosphere. The work has been concluded as follows:

- ZnS:Eu nanoparticles are found to have cubic crystal structure with the diffraction peaks coming from (111), (220), and (311) planes.
- On heat treatment of the ZnS:Eu nanoparticles, the diffraction peaks have become more intense and sharp, showing the increase in the crystallanity.
- The mean calculated crystallite size of the ZnS:Eu nanoparticles is of the order of Bohr`s Exciton radius for ZnS, 5 nm, which shows that the synthesized nanoparticles are in the quantum confinement regime. Thus, these nanoparticles may also be called the quantum dots. Moreover, the crystallite size has increased on heat treatment of the samples by a fraction of nm.
- The elemental analysis carried out by EDX shows the atomic ratio of Zn : S : Eu is 1.000 : 0.808 : 0.002.
- FTIR studies revealed the presence mercaptoethanol ($HOCH_2CH_2SH$), which has been used as the surfactant/capping agent in the synthesis of the ZnS:Eu nanoparticles. On heat treatment, no appreciable change in the FTIR spectra has been observed, which shows that the mercaptoethanol capping is intact with the ZnS:Eu nanoparticles even after the heat treatment.
- All the absorption spectra of ZnS nanoparticles show an absorpion edge around 325 nm, with a slight red shift observed after the heat treatment of the samples. The as-synthesized samples show the excitonic peak centered at around 315 nm. This is due to the quantum confinement effect. However, this excitonic peak fades away after heat treatment.

- The optical band gap values have been calculted from the differential minima of the absorbance versus energy plots. Band gap of ZnS:Eu calculated by differential minima varies from 3.8 to 4.6 eV.

- Room temperature PL spectra of the ZnS:Eu nanoparticles excited at a wavelength of 320 nm shows a near band edge emission of ZnS at 360 nm. The emission at 425 and 434 nm can be attributed to the recombination between the sulfur-vacancy-related donor and the valence band.

- The spectrum for undoped ZnS nanoparticles is broad and asymmetric, whereas on doping the nanoparticles with Eu ions, the spectra have become sharp. This shows that the Eu doping has removed the number of surface defects leading to radiative transitions.
- The blue emission centered at 485 nm and the green emission peak at 525 nm may be attributed to Eu^{2+} related emission, due to the $4f^7 \rightarrow 4f^6 5d^1$ radiative transitions. This emission discussed here, is not consistent to the red emission in alkaline earth sulphides, because the 5d excited states of Eu^{2+} ion are host sensitive and therefore, the $4f^6 5d^1$ states split due to spin-orbit coupling and crystal field [25], resulting in blue and green emissions. The emission intensity has decreased with heat treatment. Whereas there is no shift in the peak position has been observed.

References

[1] "Nanotechnology Basics: For Students and Other Learners", Center for Responsible Nanotechnology, World Care (2008).

[2] http://www.nanotechnology.com/docs/wtd015798.pdf

[3] http://www.nanoscience.com/education/overview.html

[4] Small Wonders, Endless Frontiers: A Review of the National Nanotechnology Initiative, National Research Council, Washington D.C., (2002), 5.

[5] Nanoscience and Nanotechnologies: Opportunities and Uncertainties, Royal Society and The Royal Academy of Engineering, UK, (2004), 5.

[6] The National Nanotechnology Initiative Strategic Plan, National Science and Technology Council, Washington D.C., December (2004).

[7] http://www.ringsurf.com/online/2003-structures.html

[8] National Nanotechnology Initiative 2000 leading to the next Industrial Revolution, A Report by the Interagency working group on Nanoscience, Engineering and Technology. (http://www.nano.gov)

[9] ASTM E 2456 – 06 Standard Terminology, Relating to Nanotechnology.

[10] http://www.evidenttech.com/quantum-dots-explained/quantum-dot-glossary.html

[11] http://www.nanofm.com/terms/quantum_confinement.html

[12]"Quantum Theory of the Optical and Electronic Properties of Semiconductor" ISBN 981-02-2002-2.

[13] http://www.nanoed.org/lessons/Apples_to_Atoms/AtoAch5.pdf

[14] R. Rossetti, J.L. Ellison, J.M. Gibson, L.E. Brus, J. Chem. Phys. **80,** (1984) 4464.

[15] W. Sang, Yo. Qian, J. Min, Do. Li, L. Wang, W. Shi, Yi. Liu, Solid State Commun **121**, (2002) 475.

[16] A. P. Alivisatos, Science **271**, (1996) 933.

[17] G. Cao, "Nanostructures & Nanomaterials: Synthesis, Properties & Applications.", Imperial College Press (2004).

[18] H. Ogawa, M. Nishikawa and M. Abe, Journal of Applied Physics **53,** (1982), 4448.

[19] P. Knauth and J. Schoonman, "Nanostructured Materials: Selected Synthesis Methods, Properties and Applications Springer" (2002).

[20] B. Das, S. Subramanium, and M. R. Melloch, Semiconductor Sci. Technol. **8,** 1347, (2000).

[21] C. Vieu, F. Carcenac, A. Pepin, Y. Chen, M. Mejias, L. Lebib, L. Manin Ferlazzo, L. Couraud, and H. Launois, Appl. Surf. Sci. **164,** (2000), 111.

[22] J. H. Park, J. Y. Kim, B. D. Chin, Y. C. Kim, and O. O. Park, Nanotechnology **15**, (2004), 1217

[23] V. L. Colvin, M. C. Schlamp, A. P. Alivisatos, Nature **370**, (1994).

[24] P. Yang, M. Lu, D. Xu, D. Yuan, G. Zhou, Appl. Phys. A **73**, (2001), 455–458.

[25] S. M. Liu, H. Q. Guo, Z. H. Zhang, F. Q. Liu and Z. G. Wang, Chin. Phys. Lett. **17,** (2000), 609.

[26] D. D. Papakonstantinou, J. Huang, P. Lianos, Journal of Materials Science Letters **17,** (1998), 1571-1573.

[27] S. J. Xu, S. J. Chua, B. Liu, L. M. Gan, C. H. Chew, Q. Q. Xu, Appl. Phys. Lett. **73,** (1998), 478.

[28] M. Ihara, T. Igarashi, T. Kusunoki, K. Ohno, *J.* Electrochem. Soc. **147, (**2000), 2355.

[29] W. Chen, J. O. Malm, V. Zwiller, Y. Huang, S. Liu, R. Wallenberg, J. O. Bovin, and L. Samuelson, Phys. Rev. B **61**, (2000), 11021.

[30] K. Jayanthi, S. Chawla, H. Chander, and D. Haranath, Cryst. Res. Technol. **42**, No. 10, (2007), 976 – 982.

[31] S. C. Qu, W. H. Zhou, F. Q. Liu, N. F. Chen, and Z. G. Wang, H. Y. Pan and D. P. Yu, Appl. Phys. Lett. **80,** (2002).

[32] A. Ishizumia, C.W. Whiteb, Y. Kanemitsu, Physica E **26,** (2005) 24–27.

[33] Y. L. Soo, Z. H. Ming, S. W. Huang, Y. H. Kao, R. N. Bhargava, and D. Gallagher, Phys. Rev. B **50**, (1994), 7602.

[34] W. Chen, J. O. Malm, V. Zwiller, R. Wallenberg and J. O. Bovin, J. Appl. Phys., Vol. **89,** No. 5, (2001)

[35] K. S. Rathore, D. Patidar, Y. Janu, N. S. Saxena, K. Sharma and T. P. Sharma, Chalcogenide Lett. **5,** (2008), 105–110.

[36] H. Okuda, J. Dakada, Y. Iwasaki, N. Hashimoto, C.Nagao, IEEE Trans. Consumer Electron. **36**, (1990), 436.

[37] J. P. Borah, J. Barman and K. C. Sharma, Chalcogenide Lett. **5,** (2008), 201

[38] Wells, A.F. (1984), Structural Inorganic Chemistry (5th ed.), Oxford: Clarendon Press, ISBN 0-19-855370-6.

[39] Greenwood, Norman N.; Earnshaw, A. (1984), Chemistry of the Elements, Oxford: Pergamon, p. 1405, ISBN 0-08-022057-6.

[40] H. Chander, Proc. of ASID, Phys. Rev. Lett. **11**, (2006).

[41] A. A. Bol, R. V. Beek and A. Meijerink, Chem Mater **14,** (2002) 1121.

[42] M. Debessai et al. (2009), "Pressure-Induced Superconducting State of Europium Metal at Low Temperatures". Phys. Rev. lett. **102**: 197002.

[43] CRC Handbook of Chemistry and Physics and the American Chemical Society.

[44] Kaeble E F, Handbook of X-rays, McGraw-Hill, New York, 1967.

[45] B. D. Cullity and S. R. Stock, Elements of X-Ray diffraction, 3rd edition, prentice hall, upper Saddle River, NJ, 2001

[46] T. Yurugi, I. Sukehiro, Y. Numata, K. Sykes, Hitachi Science Systems, Ltd., Oxford Instruments plc.

[47] http://www.siliconfareast.com/edxwdx.htm

[48] http://mmrc.caltech.edu/FTIR/FTIRintro.pdf

[49] http://www.thermo.com.cn/Article.aspx?ID=187

[50] http://www.kayelaby.npl.co.uk/chemistry/3_8/3_8_7.html

[51] http://www.cem.msu.edu/~reusch/VirtualText/Spectrpy/UV-Vis/uvspec.htm

[52] W. Lehmann, Journal of Luminescence, **5** (1972), 87.

[53] C. R. Kagan, C. B. Murray, and M. G. Bawendi, Phys. Rev. **B54**, (1996) 8633

[54] U. Lemmer and E. O. Göbel, S.Physik, Physikalisch Ludwig–Maximilians–Universität München, Amalienstr. **54**, 80799.

[55] C. Colvard, in Encyclopedia of Materials characterization, eds., C. R. Brundle, C. A. Evans Jr. and S. Wilson, Butterworth-Heinemann, Stoneham, MA, (1972), 373.

[56] T. H. Gfroerer, "Photoluminescence in Analysis of Surfaces and Interfaces" in R. A. Mayers (Ed.) (2000), 9209.

[57] Z. Jindal, N. K. Verma, J Mater Sci **43** (2008), 6539–6545

[58] G. Blasse, B. C. Grabmaier, "Luminescent Materials", Springer- Verlag; Berlin (1994).

[59] S. Lee, D. Song, D. Kim, J. Lee, S. Kim, I.Y. Park, Y.D. Choi, Mater. Lett. **58** (2004), 342.